



Simulation-Based Review of Selected LiDAR System Designs for Mobile Mapping

V.V. (Vishakha) Patel

MSC ASSIGNMENT
UAV specialization | MSc Systems & Control

Committee:

Dr. V.V. Lehtola
Prof.dr.ir. M.G. Vosselman
Dr.ir. M. Abayazid

December 2022

Department of Earth Observation Science
ITC Faculty
EEMCS
University of Twente



UNIVERSITY OF TWENTE. | **DIGITAL SOCIETY INSTITUTE**

Dedicated to the memory of my grandmother, Taraben, who always believed in me. You are gone but your belief in me has made this journey possible. I miss you

Acknowledgement

I would like to thank my thesis advisor Dr. Ville Lehtola, UT-ITC. Whenever I had a problem or a query regarding my research or writing, his office door was always open. He continuously allowed me to write this thesis on my own, but offered guidance when he believed I needed it. He was patient, understanding and supportive in my thinking process, and always encouraged to achieve more. I would also like to thank my committee chair Dr.ir. George Vosselman, for answering my never-ending emails and Dr.ir. Momen Abayazid for accepting to be a part of the evaluation committee.

Thank you for helping me overcome with technical challenges Aswin, your general knowledge and curiosity of aerial platforms, the intense brain storming sessions and always telling me to go back to fundamentals, when I needed to debug, will always be appreciated.

To my family, especially my parents, I appreciate your everlasting support. I could always count on you. Thank you mamma, for staying awake with me when I was low and making me laugh when I took life too seriously.

Finally I want to thank my friends, with whom I could share my study struggles. The valuable calls with Keshava, Nita and Bhanu always helped to stay positive and grounded.

Abstract

Mobile mapping is a way of obtaining accurate 3D maps of environments in a short time. A mobile mapping system is essentially a perception system consisting of LiDARs for obtaining geometrically accurate data with optional cameras and other sensors for auxiliary functions. When considering LiDARs, their composition and orientation influences the quality of data received. The configuration and number of LiDARs employed in the current mobile systems are driven by designer experience, understanding and requirements. So far, for a small mobile platforms such as an unmanned aerial vehicle (UAV), the systems have been limited to single-LiDAR configurations.

This study investigates the benefits of using multiple LiDAR in a (UAV-mounted) mobile platform. The study draws inspiration from two sources, as follows. First, mapping of indoor environments sets high requirements. There has been a step up from the single-sensor push-broom like data capture, to the fan-style LiDAR which captures in 3D. But to increase visibility and accuracy, the next step is for multi-LiDAR systems. Second, the advancement in the LiDAR technology (such as single photon LiDAR, flash LiDAR) has led to a reduction in weight, cost and power consumption of these devices, enabling new system design possibilities. It makes sense to use simulations to assess potentially useful systems. Here, ROS simulations are used, because that is a *de-facto* standard for robotics research and development.

Well-motivated LiDAR configurations inspired from state-of-the-art mobile platforms are selected and simulated in different environments. The point cloud obtained are assessed against the designed evaluation metric. The evaluation is based on coverage, homogeneity and normalized density of the point cloud.

Depending on the quantity of LiDARs employed, the configurations have been classified into three tiers. While examining the outcomes, certain tendencies become apparent. The point cloud's quality is directly influenced by the LiDAR system's range and direction. For different environment uses, optimal or possibly improved designs are recommended within each Tier. The designed evaluation metric serves as a suitable starting point for developing new combinations. And an important trade-off between scanning more thoroughly and flying farther is comprehended. This trade-off is crucial in defining the configuration's design and feasibility.

Contents

Acknowledgement	3
Abstract	4
1 Introduction	10
1.1 Problem Definition	10
1.2 Research Contributions	12
1.3 Outline	12
2 LiDAR Configurations	13
2.1 Operational Principles of LiDAR	13
2.2 Literature on LiDAR	14
2.3 Review of the LiDAR configurations	15
2.4 Proposed Configurations	17
3 Metric for Point Cloud Quality Assessment	21
3.1 Literature on Point Cloud Quality	21
3.2 Evaluation Metric	22
3.2.1 Nominal Point Cloud Density	22
3.2.2 Homogeneity Score	23
3.2.3 Accuracy and precision	24
3.2.4 Coverage	24
4 Simulator Tool	26
4.1 Literature on simulator	26
4.2 Building the Environment	27
4.2.1 Warehouse Environment	27
4.2.2 Medical Camp	28
4.2.3 Forest	29
4.3 Simulating the Platform	30
5 Results	33
5.1 Warehouse	33

5.1.1	Visual Analysis	33
5.1.2	Nominal Point Density and Homogeneity Score	36
5.1.3	Coverage	36
5.2	Medical Camp	36
5.2.1	Visual Inspection	36
5.2.2	Nominal Point Density and Homogeneity Score	42
5.2.3	Coverage	42
5.2.4	Range and Orientation of LiDAR	45
5.3	Forest	47
5.3.1	Visual Analysis	47
5.3.2	Nominal Point Density and Homogeneity Score	52
5.3.3	Coverage	52
6	Discussion	54
6.1	Discussion	54
6.2	Complexity and Limitations	58
6.3	Future work	58
7	Conclusion	60
7.1	Summary of Research Contribution	61
	References	62

List of Figures

2.1	Flash LiDAR capturing	14
2.2	Mobile Mapping Aerial Platforms	16
2.3	Mobile Mapping Platforms	17
2.4	Tier 1 Configuration - single LiDAR	20
2.5	Tier 2 Configuration - Dual LiDAR	20
2.6	Tier 3 Configuration - 3 or more LiDAR	20
3.1	Local Point Cloud Density	23
3.2	Standard deviation of a point cloud with Gaussian distribution	24
4.1	Ground truth point cloud of warehouse environment with its trajectory	27
4.2	Spatial distribution of points in warehouse environment	28
4.3	Ground truth of Medical camp environment displayed with the trajectory	29
4.4	Spatial distribution of points in medical camp environment	29
4.5	Ground truth point cloud of forest environment, displayed with height colouring	30
4.6	Trajectory followed by the platform in the forest environment	31
4.7	Spatial distribution of points in Forest environment	31
5.1	Point cloud section of a warehouse as captured from configuration 1 (VLP front)	34
5.2	Reference point cloud section of <i>Europallet</i>	34
5.3	Point cloud section of Configuration 2, depiction shadowed regions	34
5.4	Point cloud section of Configuration 3, depiction fuzzy data	35
5.5	Point cloud section recorded by Configuration 4	35
5.6	Point cloud section of scan pattern seen for VLP16 LiDAR	37
5.7	Point cloud section of <i>Reception</i> model seen for VLP16 LiDAR	37
5.8	Point cloud section of a room in hospital captured from configuration 3	37
5.9	Difference in point cloud recorded by configuration 1 and 5	38
5.10	Difference in shadowed region from point cloud recorded by configuration 2 and 6	38
5.11	Point Cloud section of Configuration 4 showing untraveled corridor	39
5.12	Point Cloud section of Configuration 5 showing untraveled corridor	39
5.13	Point Cloud section of Configuration 6 showing untraveled corridor	39
5.14	Point cloud simulated from configuration 8	40

5.15	Point cloud simulated from Configuration 9	40
5.16	Point cloud section used to calculate cut-off distance	43
5.17	Graph of Coverage vs cutoff distance	44
5.18	Coverage point cloud for Configuration 7, Yellow points are unscanned regions, and Blue points are scanned regions	44
5.19	Point cloud coverage for each configuration in the medical camp environment	45
5.20	Single LiDAR mounted on a small mobile platform with changing orientation .	46
5.21	Section of forest point cloud, considered for reference	47
5.22	Comparison of top view of point cloud as seen from c1 (blue) and c2 (green) . .	47
5.23	Point cloud obtained from configuration 1	48
5.24	Point cloud obtained from configuration 2	48
5.25	Point cloud obtained from configuration 3	49
5.26	Point cloud obtained from configuration 5	49
5.27	Point cloud obtained from configuration 6	49
5.28	Point cloud obtained from configuration 7	50
5.29	Point cloud obtained from configuration 9	50
5.30	Point cloud coverage for each configuration in the forest environment	53
6.1	Summary from evaluation metric	55

List of Tables

2.1	Commonly used LiDAR on a mobile platform	15
2.2	Sensor specification used for Simulation	18
2.3	The sensors and their orientation on the small mobile platform for the proposed designs	19
5.1	Nominal Point density and Homogeneity score for warehouse environment, red highlighting the poor score and green for the best score	36
5.2	Visual Analysis for medical camp environment	41
5.3	Nominal Point density and Homogeneity score for medical camp environment, red highlighting the poor score and green for the best score	43
5.4	Coverage calculated for different range of LiDAR	46
5.5	Nominal point density and Coverage for change in inclination of a single LiDAR (<i>VLP16</i>) in medical camp environment	46
5.6	Visual Analysis for forest environment	51
5.7	Nominal Point density and Homogeneity score for forest environment, red highlighting the poor score and green for the best score	52

Chapter 1

Introduction

The advancement in LiDAR technology is re-shaping the LiDAR perception system used in a Mobile mapping system (MMS). MMS systems are capable of providing accurate, efficient and fast results which enable its applications in construction sites, forest and agriculture, hospital or medical sector, mining and tunnels, road, railway and bridge inspection. Depending on the application of the mobile mapping system there are various 'mobile platforms' used such as car, drone, backpack to collect geospatial information. The commonly used sensors for perception on a MMS platform is LiDAR (Light Detection and Ranging), or camera. Positioning modules like IMU (Inertial Measurement Unit) can be used to position the mobile platform for indoor environments, although IMU data is subject to drift. Data from the perception module (LiDAR data) can be co-related with the IMU data to better localize the system and minimize drift. Since the accuracy of this depends on the perception system, it becomes crucial to determine the orientation and number of LiDARs used.

A point cloud is a set of data points in a three-dimensional coordinate system. These points are typically generated by a laser scanning device, and they can be used to create 3D models of objects or environments. Point clouds are often used in fields such as surveying, architecture, and engineering. The point clouds can be colored according to the intensity, ring or height values. Certain point clouds can contain the color and light intensity of the measurement point in addition to the XYZ coordinates. Each point can also be given a direction vector, which identifies the direction in which the point is oriented.

1.1 Problem Definition

Over the past years, 3D LiDARs have improved and grown with attention. The investment in it by industry players, shows a promising future in LiDAR technology. The innovation of single photon LiDAR (or flash LiDAR) have reduced the size and complexity in the designs. This encourages us to explore the possibility of increasing the LiDARs on a given platform.

Even with the immense development in LiDAR technology and integration with MMS, there is not much information provided on the number and orientation of LiDAR to be used. Engineers and developers depend on their prior knowledge for deciding the configuration of the perception system, along with the system requirements. It is necessary to study the existing LiDAR systems, and the benefits they provide.

To assess the existing systems, an evaluation metric has to be designed which can assess the quality of the system designs. A quantitative assessment to system design would be the evaluation of the point cloud quality generated from the different LiDAR set-ups. A qualitative assessment would include external factors such as cost, design complexity, LiDAR power consumption. It becomes important to understand the factors influencing the trade-off between scanning harder (quantitative assessment) or flying longer (qualitative assessment). There are several ways to assess the quality of point clouds generated by LiDAR. One common approach is to compare the point cloud with a known reference, such as a high-resolution 3D model or a ground truth point cloud. This allows one to measure the accuracy and completeness of the point cloud. Another way to assess the quality of a point cloud is to look for potential errors or artifacts, such as missing points, noise, or outliers. In general, a high-quality point cloud will accurately represent the geometry of the objects or environment being scanned, and it will be suitable for use in a variety of applications.

On understanding the significance of the existing LiDAR design configurations, new designs can be proposed. The evaluation of the new design will be against the metric designed previously. This will give insights on the viability of increasing the number of LiDARs, the improvement in orientation and the specification on the trade-off between scanning harder or flying longer. The new designs proposed have to be explored and an improvement on the existing designs, if any.

The development of a simulation tool is essential to test out the new design configurations and their feasibility. It is inexpensive to test it on a controlled simulated environment. A simulated environment, also reduces the complexity of variables. It is not feasible to experiment in reality with N LiDARs due to hardware, cost, set-up design restrictions without any positive results. Moreover, such experiments are difficult to execute as all equipment have to be brought to a single location, and one has to scout a good testing environment.

The new design configurations, have to be tested under different application scenarios. This helps in understanding the overall performance of the designs with each other, and under contrasting circumstances. The comparative analysis of the state-of-the-art and newly proposed designs, will also aid in determining factors which effect the evaluation metric. With a comparative analysis, it will be possible to determine an optimal configuration, if any, or a replaceable configuration to one other. This provides motivates to explore the difference in point clouds generated with different orientations of LiDAR, and if increase in the number

of LiDAR is efficient or redundant.

1.2 Research Contributions

This work contains the following research contributions:

- Review of the selected state-of-the-art LiDAR systems mounted on small mobile platforms.
- Appraising and designing evaluation metrics for assessing the quality of selected systems.
- Proposing new system designs based on the state-of-the-art review.
- Building of a tool for simulating the selected systems in controlled test environments
- Comparative analysis of the state-of-the-art and newly proposed LiDAR system designs in different simulated environments

1.3 Outline

The rest of the work is organized as follows. Chapter 2 provides the working principal of laser scanners with a literature study, along with a review of the selected state-of-the-art LiDAR mounted small mobile platforms and new design configurations proposed. Chapter 3 introduces the evaluation metric utilized for the assessment of the point cloud quality. Chapter 4 explains the pipeline used to build the simulating tool in ROS and Gazebo, along with the environments explored for simulation. Chapter 5 presents the results for the three environments explored along with a brief insight on the configurations. Chapter 6 discussed the insights obtained from the results presented, with limitations, complexity and possible future works. Chapter 7, concludes the discussions on the results presented and summarizes the research contributions of the thesis.

Chapter 2

LiDAR Configurations

2.1 Operational Principles of LiDAR

LiDAR is an acronym on Light Detecting and Ranging, as it uses light to measure the distance to an object. LiDAR works in a similar manner as a RaDAR or SoNAR, except it uses light waves to travel. LiDAR consists of a emitter and receiver. The emitter emits pulsed light (laser pulses) towards a target and then measures the time it takes for that light to strike back. The distance is then calculated according to Eq2.1 :

$$d = \frac{c \times \Delta T}{2\eta} \quad (2.1)$$

where c is the speed of light, ΔT is the time between the emitter emits the pulse and the receiver receives it, and η is refractive index of propagation medium which is 1 for air.

As the mobile platform moves, the LiDAR will emit multiple pulses to map out its surrounding and return a 3D point cloud. LiDAR has several advantages in capturing data. It provides accurate, fast and in-depth images. Light rays can penetrate an occluded (cloudy scene), which a camera can not capture. But on the downside, it does not capture texture or colour which could mean difficulty in interpreting data. But post-processing on point cloud data, has made this easier, Martin Velas et al. Velas et al. 2019 uses a novel approach that assigns colour to the points with normalization of intensity. The intensity is affected by the reflection from the surface, the incident angle, distance from the laser (emitter). They have developed an approach which helps in easy distinguishing of important features, surface texture and inventory. Besides this improving downside, LiDAR is expensive, provides with too much data. This excess data requires good back processing and knowledge.

2.2 Literature on LiDAR

LiDAR specification is essential to a designer and developer, depending on the application. Raj et al. 2020 classifies the specification into 4 levels of a hierarchy format. The first level of classification is ranging specification, this includes range, resolution, field of view (FoV), angular resolution, update frequency, this is important during indoor/outdoor navigation where long range or short range lasers are required. The second class consists of physical properties such as weight, height and power consumption. This attribute is important to consider while mounting the laser on a mobile platform such as an aerial vehicle. The third class of classification is the laser safety compliance and the last is related to optics such as focal length of the beam. Raj et al. 2020 explains the different scanning methods available. This can in general be classified as mechanical scanning (LiDAR which has a motor rotating part), MEMS scanning use electromagnetic force to rotate a micro chip (mirror) to produce a dense point cloud. This reduces the overall weight of the scanner but also has a restricted FoV and finally the solid-state scanner which work as a flash LiDAR thereby reducing the size a lot further and reducing the cost as well.

The concept of flash LiDAR is emerging, and promising. The traditional 3D LiDAR such as Velodyne's VLP16 or HDL32 use 16 or 32 lasers that are stacked in a vertical array and a motor rotates the mirror of the laser beam at a high speed (5Hz-20Hz) thus obtaining a 360deg FoV, providing a dense point cloud data. On the other hand flash LiDAR work on the concept similar to a camera flash. Thereby illuminating the entire surface by a flash of light. This captures the surface illuminated in one go (global shutter flash), as seen in Fig.2.1¹. The range of flash LiDAR is small compared to scanning LiDAR.

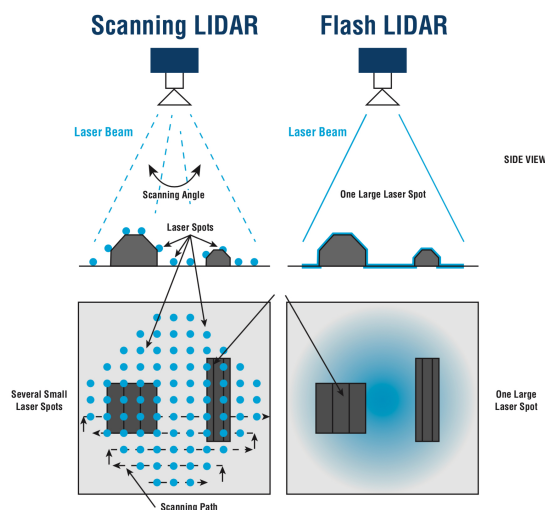


Figure 2.1: Flash LiDAR capturing

¹<https://asc3d.com/our-technology/>

A survey of 3D flash LiDAR is presented in Yang et al. 2022. Flash LiDAR uses a photo-diode as its receiver. This questions the working conditions of the LiDAR on a sunny bright day. The application in last-mile delivery, indoor environments, warehouse inventory and health care monitoring looks promising.

The focus of this thesis will be on simulating a mobile platform consisting of an Unmanned Aerial Vehicle. To the author's knowledge there does not exist an aerial platform with more than one LiDAR configuration. There have been development in backpack as a mobile platform with different LiDAR orientation. Velas et al. 2019 proposed two LiDAR orientated inclined to each other similar to a wedge setup. S. Karam, V. Lehtola, and Vosselman 2020 integrates three scanners with a Xsense IMU. The lack of increasing the number of LiDAR on an aerial platform can be because LiDARs drain power quickly, and Aerial platform provide 6DoF making it easy to maneuver. But with the improvement and a promising future in Flash LiDAR, this track is worth exploring.

The commonly used LiDARs on an Aerial² Platform are listed in Table2.1.

Model	Type	Max Range (m)	FOV H° × V°	Cost
Velodyne VLP16	Scanning	100	360 × 30	\$\$
Velodyne HDL32E	Scanning	100	360 × 40	\$\$\$
LeddarTech Vu8	SS ³	215	48 × 3	\$\$
Riegl VUX-1UAV	Scanning	250	330	\$\$
TeraRanger Evo 15m	Flash	15	2	\$
Velodyne Alpha Prime	Scanning	265	360 × 40	\$\$\$
Ouster OS1	Scanning	120	360 × 45	\$\$\$
Velodyne Velarray M1600	Flash	30	120 × 32	n/a

Table 2.1: Commonly used LiDAR on a mobile platform

2.3 Review of the LiDAR configurations

The inspiration for the different design configurations has been drawn from the various available aerial systems as seen in Fig.2.2. The most commonly used LiDAR sensor on an aerial platform is observed to be the "fan-style" LiDAR which provides a horizontal field of view (HFoV) of 360° and a limited vertical field of view (VFoV). The difference in the platform is the orientation of the 360° *fan-style* LiDAR. As seen in Fig.2.2a, The *Flyability Elios 3* mounts the LiDAR in an inclined way, for indoor mapping and inspection. The *Hovermap ST* (Fig.2.2b) has a rotating mount which provides 360° × 360° FoV. This drone is capable of

²And other commonly used LiDAR in Robotics

flying indoor or outdoor. The *Revolution Drone System* uses *DJI Matrice 600 Pro Drone* with the *Velodyne HDL32e* LiDAR. It provides a robust solution for mapping through the woods. The *Acecore Zoe* by YellowScan, utilizes their own LiDAR system and offer a complete package.



Figure 2.2: Mobile Mapping Aerial Platforms

The inspiration for different configurations has not been restricted to only the aerial platforms, but also includes inspirations from other mobile mapping systems as seen from Fig.2.3. The *Terabeer TeraRanger* (Fig.2.3a) provides an option to mount the LiDARs as individual or in a combination. It uses flash LiDAR having a FoV of 2° . The *Velodyne Velarray Cart* utilizes *Velarray M1600* LiDAR having a HFoV of 120° and VFoV of 32° . It can supply the intelligent, real-time point clouds necessary for last-mile delivery and autonomous mobility robots to operate safely and for an extended period of time without human interaction. Fig.2.3b shows another Velodyne mobile platform, which utilized the *HDL-32E*. *Waymo* which is the *Google Self Driving Car* has a similar set up of a 360° LiDAR placed on top of the moving platform. The *Trimble MX9* (Fig.2.3d) is a complete set-up that utilizes two 'fan-style' LiDAR. This setup is meant for a moving platform as a vehicle. The last two set-ups are essentially used with big mobile platform that can have more storage for batteries, but the study here is considered on small mobile platforms. Keeping this in mind, these two set-ups are used only as an inspiration to design configurations that can be set-up on a small

platform.



(a) Terabeer TeraRanger Tower Evo 60m



(b) Velodyne DeepMap



(c) Velodyne Velarray Cart



(d) Trimble MX9

Figure 2.3: Mobile Mapping Platforms

2.4 Proposed Configurations

The inspiration drawn for the platform has been discussed previously. The configuration designs are divided into 3 tiers according to the number of LiDARs on the platform. *Tier 1*, as seen in 2.4 consists one one LiDAR, in different orientation. This is easily accessible and commonly seen around on small mobile platforms. The *Tier 2*, seen in 2.5, consists of two LiDAR on a platform, this is a further modification from *Tier 1*. *Tier 2* can be observed as a combination of *Scanning LiDAR* and *Flash LiDAR*⁴. The next, *Tier 3*, as seen in 2.6 consists of 3 or more LiDARs. The configurations here are entirely fictional and not seen before. All configurations are decided keeping in mind few important features of a LiDAR.

- FoV - The angle that the LiDAR sensor covers, is known as the field-of-view. The LiDARs have a horizontal FoV and a vertical FoV. Spinning LiDAR offer a complete 360° view, the vertical FoV is dependent on the spacing of the lasers stacked on another.

⁴Dark blue triangle are the HFoV of 120° and light blue colour is VFoV of 32°

For a LiDAR with a given number of lasers, narrower FoV will give a denser point cloud compared to a widespread vertical FoV.

- **Range** - The distance up-to which the laser lights can detect, is the range. This depends on the wavelength of the laser pulse used. Usually, the scanning LiDAR have a longer range, when compared to the flash LiDAR which have a short range.
- **Point frequency** - Point frequency is the number of horizontal rotating samples. Increasing the point frequency, increases the point density linearly. Modern LiDAR have multiple lasers or channels, that can produce a very high dense point collection of up-to 2.2 million points per second (Vectornav n.d.). A high density of points can break the simulation environment. The point frequency or samples, have been restricted to 100 samples, keeping in mind increasing this value only gives a denser point cloud.
- **Scanning frequency** - Scanning frequency is the rotation of the LiDAR scanner head per second. The VLP-16 and HDL32e have a scanning frequency of 5Hz - 20Hz. For the simulation here, the scanning frequency for the scanning type LiDARs is fixed to 10Hz. The flash LiDAR does not have a scanning frequency. The frame rate for Flash LiDAR is the frequency with which the LiDAR acquires the forward point cloud image in a second.

The sensor (or fictional sensor) used in the set-up are listed below ⁵

LiDAR	Laser	HFoV	VFoV	Range	Cost	Power Consumption	Weight
HDL32E	32	360°	41°	100m	\$\$\$	●	1kg
VLP16	16	360°	30°	130m	\$\$	◐	830g
Velarray M1600	Flash	120°	32°	30m	\$	◑	n/a

Table 2.2: Sensor specification used for Simulation

⁵The weight of Velarray was not available, but in general Flash LiDARs weigh a few grams

Config	HDL32E (H)	VLP16 (V)	Velarray (M)	Orientation [r p y]
1	x	1	x	V:[0 90° 0]
2	x	1	x	V:[0 45° 0]
3	1	x	x	H:[0 0 0]
4	1	1	x	H:[0 0 0]; V:[0 90° 0]
5	x	1	1	V:[0 90° 0]; M:[0 0 0]
6	x	1	1	V:[0 45° 0]; M:[0 180° 0]
7	1	x	2	H:[0 0 0]; M1:[0 135° 0]; M2:[0 -135° 0]
8	1	1	1	H:[0 0 0]; V:[0 90° 0]; M:[0 135° 0]
9	x	x	4	M1:[0 135° 0]; M2:[0 -135° 0]; M3:[0 45° 90°]; M4:[0 -45° 90°]

Table 2.3: The sensors and their orientation on the small mobile platform for the proposed designs

Configuration 1 consists of VLP16 laser oriented with the scanning axis parallel to the ground. This is a common practice, Lassiter et al. 2020 explores the importance of this orientation and also mathematically provides an equation for the scan pattern of the fan-style LiDAR. The scan lines are then parallel to the direction of travel. Configuration 2 has the VLP LiDAR tilted by 45° down from the scanning axis. Configuration 3 is a HDL32e LiDAR mounted in an upright position. Configuration 4 is a combination of c1 and c3. Configuration 5 has the additional Flash LiDAR (Vellarray) in combination with c1. The flash LiDAR is placed on the opposite side of VLP. The dark blue triangle represents the vertical FoV, the light blue triangle represents the horizontal FoV. Configuration 6 is a modification of c2 with the flash LiDAR facing down (such that the scan lines are perpendicular to direction of travel). Configuration 7 is a modification on c3, the two flash LiDAR are placed at the opposite side of the mobile platform, with a 45° downwards tilt. Configuration 8, consists of all three LiDARs, it is a modification on c4, with the flash LiDAR tilted 45° downwards. Configuration 9, is a different configuration consisting of all flash LiDARs. They are placed such that one pair (opposite LiDARs) is tilted down by 45° and the other pair is inclined by 45° upward.

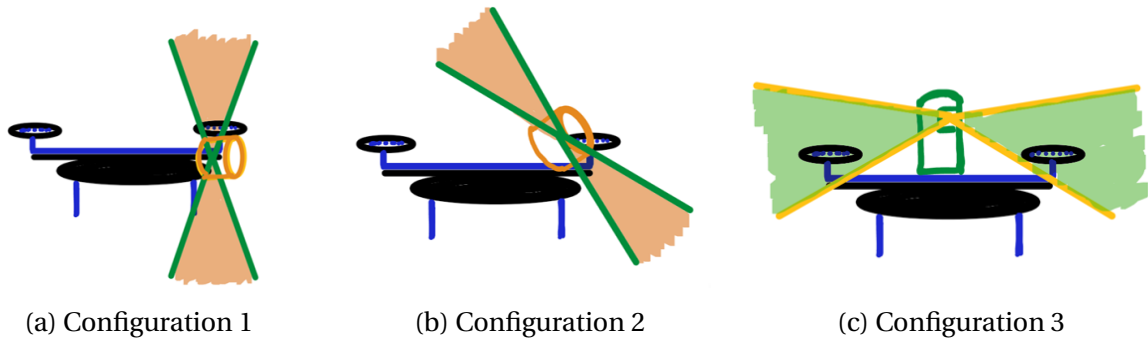


Figure 2.4: Tier 1 Configuration - single LiDAR

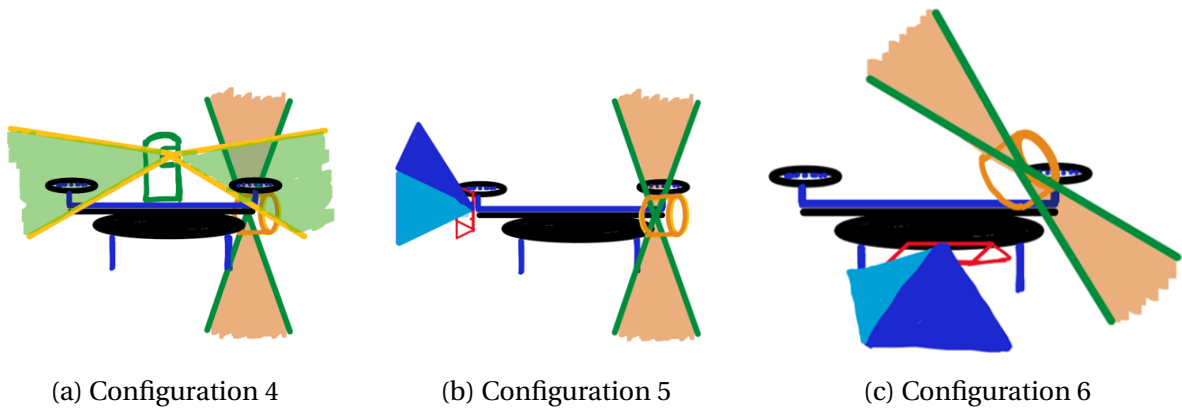


Figure 2.5: Tier 2 Configuration - Dual LiDAR

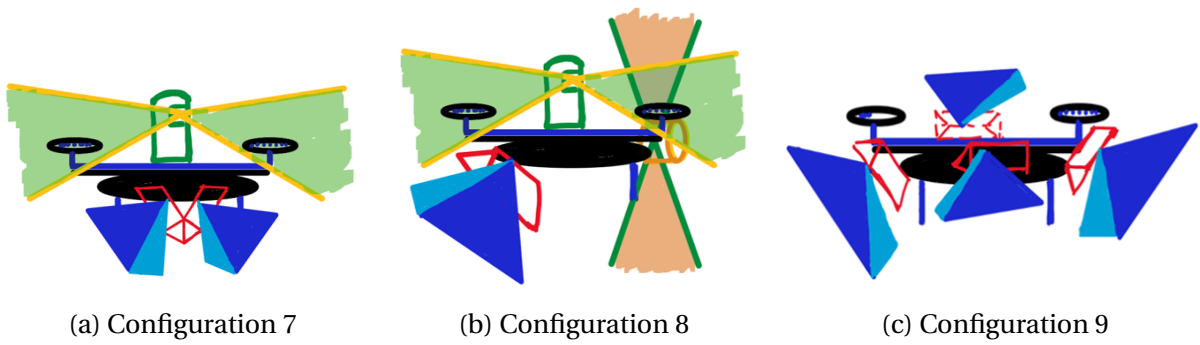


Figure 2.6: Tier 3 Configuration - 3 or more LiDAR

Chapter 3

Metric for Point Cloud Quality Assessment

3.1 Literature on Point Cloud Quality

Point clouds represent collection of co-ordinates in space. Each point point is defined by its own position. A LiDAR produces an extensive collection of point cloud data of accurate measurement. It is important to understand the quality of a point cloud. Khoshelham et al. 2021 defines a metric for evaluating point cloud completeness, correctness and accuracy. These metrics are defined considering a reference and a reconstructed point cloud to a mesh. The portion of the reference surface that are present and have been correctly recreated in the source is termed correctness and completeness respectively. Accuracy is the measure of proximity of the source to the reference surface. It is calculated using the distance and direction between the normal.

Ville Lehtola et al. 2017 provides a metric for point to point comparison (p2p) from rigid environments. L1 or L2-norms, with a cut-off distance, can be used as a metric for evaluating raw point cloud data. They introduce a cut-off radius r_c is introduced to define completeness of the point cloud. The cut-off radius is a trade-off between a strict measurement or including outliers. The error matrix E is defined as a function of cut-off radius. And the point where E saturates, is the critical point for cut-off. The function E rises due three essential reasons. Firstly, outliers in the compared point cloud, secondly, it covers a larger area than the reference and third would be deformation or internal registration errors in reference point cloud.

Point-to-point comparison frequently overlooks the fact that a point cloud represents a structure's surface (texture). To overcome this, Tian et al. 2017 a point-to-plane approach is introduced. It first employs point-to-point calculation (Euclidean distance) to compute the error vector, and then employs point-to-plane calculation to project the error vector along the normal direction of the reference point. The visual qualities of the point cloud are preserved with this metric.

Another metric for assessing the correlation between the reference and source point cloud is plane-to-plane comparison. This is described in Alexiou and Ebrahimi 2018. This plane-to-plane comparison provides angular similarity between the two point cloud. The angular similarity is calculated using the Euclidean distance, thereby finding the nearest neighbour between the two point clouds. The angle is calculated between the tangent plane of the respective point clouds. The normal vector is required to be present while calculating angular similarity.

All comparison measures are based on point-to-point, point-to-plane, or plane-to-plane measurements. Yoo et al. 2009 presents an evaluation index consisting of criteria such as *Resolution* or *Density*, a score on *Homogeneity* and *Completeness*. These scores evaluate different Laser Scanner configuration on a mobile mapping system for a specific application of "Architecture for 3D tourism". The completeness is not evaluated against a quantitative evaluation, but depends on a visual inspection of the point cloud.

Cahalane et al. 2015 demonstrates the benefit of a dual scanner system. A horizontal rotation of the scanner is responsible for the range, where as vertical rotation gives an advantage in scanning profiles. The orientation of the Laser scanner directly influences the point density and profile distribution.

3.2 Evaluation Metric

The evaluation metric is an assessment of *Nominal Point Density*, *Homogeneity score* and *Coverage*. The evaluation here is to assess the quality of point cloud obtained from the different configuration in complex environments.

3.2.1 Nominal Point Cloud Density

The point cloud density ρ_D , is dependent on the platform speed, and laser specifications. Simulations are carried out at a constant mobile platform speed of $5cm/s$ and the mobile platform is at a constant height from ground. This allows the platform variables to be treated as constants, and the point density function can focus on LiDAR specifications for calculations. Point cloud density is calculated as the number of neighbouring points per unit area (sphere) for each coordinate point. From Fig.3.1 the red point is the reference point. And points within the sphere of radius r are the neighbouring points. The yellow points, outside the sphere are non-neighbouring points. The point density can be expressed as volume density in pts/m^3 or surface density in pts/m^2 . Here, the point density is expressed as a volume density in pts/m^3 . The mean density $\bar{\rho}$ is the sum of indices of all local point densities ρ_i , where number of points are n_T .

$$\bar{\rho} = \frac{1}{n_T} \sum \rho_i \quad (3.1)$$

The nominal density of the point cloud is calculated keeping the point frequency, and as mentioned before the platform speed and height constant for simulations in every environment. The *nominal point density*, ρ_D here, is defined as the ratio of logarithmic mean density ($\bar{\rho}$) of simulated point cloud to the reference point cloud. The logarithmic function (to base 10) is used to scale down the high mean density value. The reference point cloud has a mean density of ranging from 10^4 to 10^5 pts/m^3 . Since NPD is defined as a ratio, it does not have a *unit*.

$$\rho_D = \frac{\log_{10}(\bar{\rho}_{sim})}{\log_{10}(\bar{\rho}_{ref})} \quad (3.2)$$

The density of simulated point cloud is compared to the reference point cloud build according to the collision of each and every individual model present in the worlds.

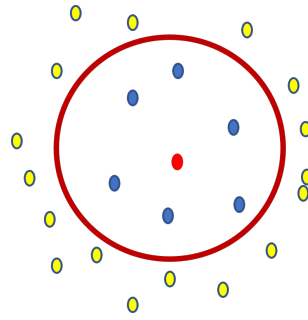


Figure 3.1: Local Point Cloud Density

3.2.2 Homogeneity Score

If all point densities are the same, then the data is homogeneous. Homogeneous data has a standard deviation $\sigma = 0$. but for a mobile mapping system, data produced is not going to be homogeneous. If the system is turning left, the left side will be over-dense, and the right will be under-dense. Under-density will result in missing data, and over-density will give redundant data. Post processing of data will provide a more uniform point cloud, but will depend on the lower limit of the part of point-cloud which is under-dense. Fig.3.2 depicts the local point density distribution for a configuration in a simulated environment. The thick red red line, is the mean of the local point density, and the dotted red line is the standard deviation of the data. The further away the dotted line, higher is the standard deviation σ . It will be interesting to observe if an additional LiDAR sensor changes the homogeneity of a point cloud. The score of homogeneity is defined below.

$$\chi = 1 - \frac{\sigma}{\bar{\rho}} \quad (3.3)$$

When $\sigma = 0$, the point cloud is homogeneous, and the homogeneity score, χ is 1.

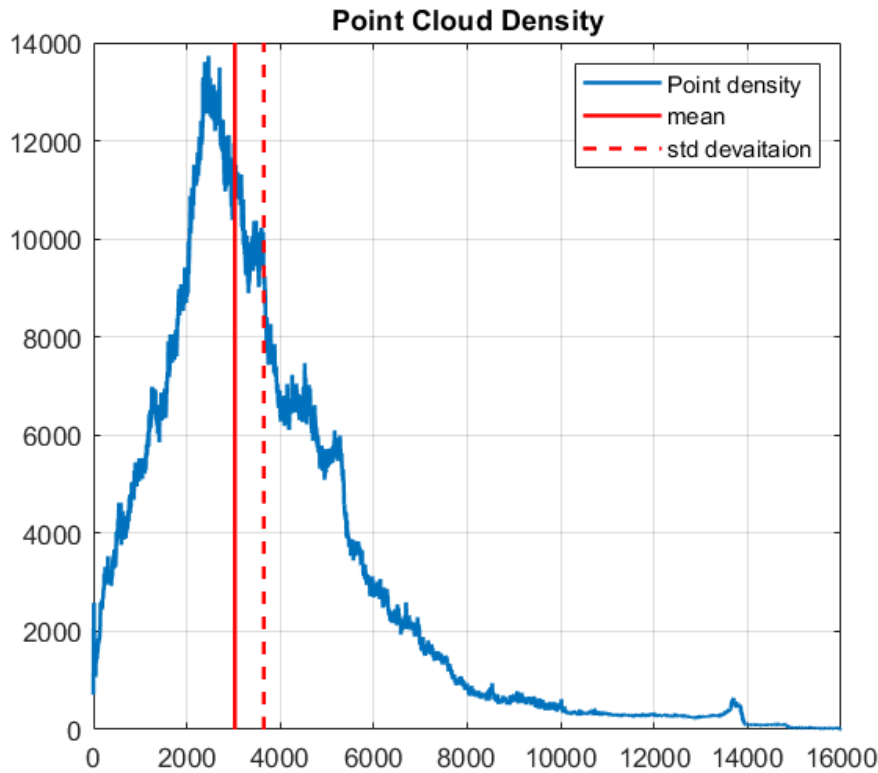


Figure 3.2: Standard deviation of a point cloud with Gaussian distribution

3.2.3 Accuracy and precision

The closeness in measurement of the simulated data with the reference data. But since noise is not modulated in simulation, it is assumed the simulation provides accurate and precise data. The score for this is not included.

3.2.4 Coverage

Depending on context, completeness or correctness communicate comparable analysis. It is the proportion of the simulated cloud that can be reconstructed with the reference. Since, this thesis does not enter the territory of re-constructing meshes or surface from point-cloud, a new term called *coverage* is coined. Coverage is defined as the portion of the original point point cloud that the simulated point cloud covers.

Consider point cloud A to be the reference point cloud, created from the collisions of the models present in the Gazebo world. And point cloud B to be the simulated point cloud. For each point of $a_i \in A$, the closest point in B is b_{jm} and can be calculated using the Euclidean distance. This error in distance is defined as $e_{A,B}$.

$$[e_{A,B}(i), b_{jm}] = \min_{\forall j \in B} \|a_i - b_j\|_2 \quad (3.4)$$

The error $e_{A,B}$ is compared against a *cutoff* distance d_c . This is a tricky part, because the cut-off distance is a trade off value. A relatively small cutoff distance would lessen the impact of feature details, whereas a high cutoff distance would be tolerant of outliers. Cut-off distance has to be chosen with care. With the cut-off distance chosen, there is another check required which ensures the point is actually covered, and not a pseudo single point present. The simulated point cloud, is divided into smaller grid (approx $10cm \times 10cm$), such that each grid box, contains a range of point from 0 - 20. It is considered that a minimum of two points are required for coverage. If the number of points inside the grid N_{inside} is 2 or more, the point is considered 'to be covered'. Detail algorithm is explained in 1, where n_A is the total number of points in reference point cloud **A** and n_B is the total number of points in simulated point cloud **B**.

Algorithm 1 Algorithm for calculating Coverage

Require: $n_A \geq n_B$

- 1: Load reference point cloud **A** and simulated point cloud **B**
 - 2: Divide point cloud **B** into smaller grid. Calculate the *grid-id* and N_{inside}
 - 3: Calculate the Euclidean distance or error between point cloud **A** & **B** according to eq.3.2.4
 - 4: **while** $a_i \leq n_A$
 - 5: **if** $error(a_i) \geq d_c$ **then**
 - 6: Point (a_i) is further away. Set **pt.Color** = *yellow*
 - 7: **else**
 - 8: **if** $N_{inside}(a_i) \geq 2$ **then**
 - 9: Point is covered. Set **pt.Color** = *blue*, update Coverage counter
 - 10: **else**
 - 11: Point not covered. Set **pt.Color** = *yellow*
 - 12: **end if**
 - 13: **end if**
 - 14: Update a_i
 - 15: **end while**
-

Chapter 4

Simulator Tool

The Gazebo is a open-source, well-recognized platform in industries and education for developing realistic 3D scenarios of robots in indoor and outdoor environments. The Gazebo environments are called as worlds. And it also has the ability to simulate different types of sensors (such as LiDARs, IMU, camera) and collect the data required for navigation. The sensor data collected can be visualized on Gazebo or Rviz. These features of Gazebo help in building custom worlds or modifying the worlds available. This project will use Gazebo to construct a warehouse environment, utilise the medical camp environment available on *aws-robotics*¹, and explore a brief forest environment constructed from different trees placed close together.

Gazebo is integrated with ROS, which is supported by the Open Source Robotics Foundation. ROS works with many different programming languages (Python, C++, Java) making it an effective tool for creating autonomous robots. The integration of the sensors, with their plugins and libraries in ROS makes it streamlined in the development of the autonomous system.

4.1 Literature on simulator

Mobile Mapping Systems that have implemented different LiDAR configurations (Velas et al. 2019, S. Karam, V. Lehtola, and Vosselman 2020) have been tested in a physical set-up and not a simulated one. Chung et al. 2017 has developed a simulator for a backpack system tested in indoor environments. Simulation is carried out using three different LiDAR (VLP16) arrangements. The simulation workflow defined is basic and starts off with modelling the sensor specification, organizing the simulation environment, followed by setting up the pathway and collecting the result as a 3D point cloud. Qualitative and quantitative analysis is performed on the data. They compare the coverage of the point clouds obtained

¹<https://github.com/aws-robotics>

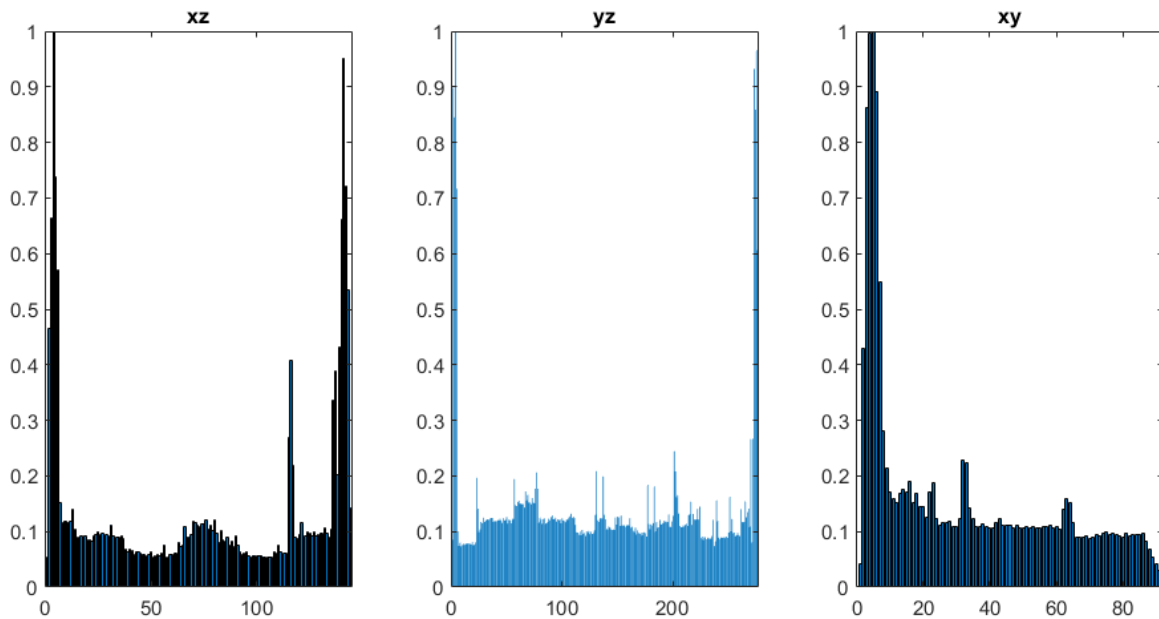


Figure 4.2: Spatial distribution of points in warehouse environment

4.2.2 Medical Camp

The Medical Camp is an inspired environment from the Gazebo worlds *aws-robotics/hospital*. Medical assistance is given high priority in a crisis situation. However, crowding a disaster-prone location with too many people is dangerous and chaotic. After a disaster, medical camps that are built nearby can be controlled using a small mobile platform. It will increase productivity and lessen the possibility of putting human lives at jeopardy at such a crucial location. In this situation, mobile platforms can aid the nurse with their work by delivering medications and meals to the appropriate bed tray (patients). It is essential to keep updating every little information in the map since the medical camp is a crucial location and is always changing as patients in wheelchairs being assisted, stretchers are being pushed out, and people are moving around. The perception system requires to be able to register all details quick and efficiently. The platform is at a height of $3.4m$ from the ground. The camp is a bigger environment and has a complex trajectory. The trajectory chosen here is such that the mobile platform fully enter some room patrolling in it, partially enters other rooms such as crossing through it, and does not at all enter the other rooms. This provides us with different data, even about rooms that have not been entered. The spatial distribution of data can be seen in Fig.4.4. The environment is divided into bins of $10cm$ for each plane (xz , yz and xy). A high density of points is seen in the xy plane. The xz and yz plane show a high density at bins corresponding to walls, beds and other object located in the environment. The spatial distribution is similar to that of the *warehouse* environment.

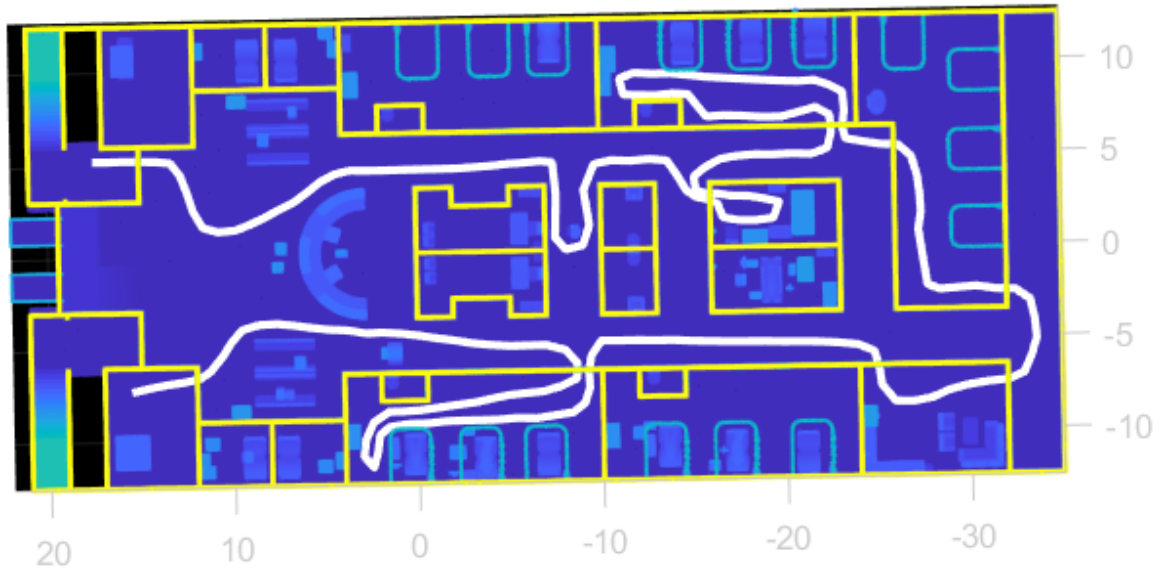


Figure 4.3: Ground truth of Medical camp environment displayed with the trajectory

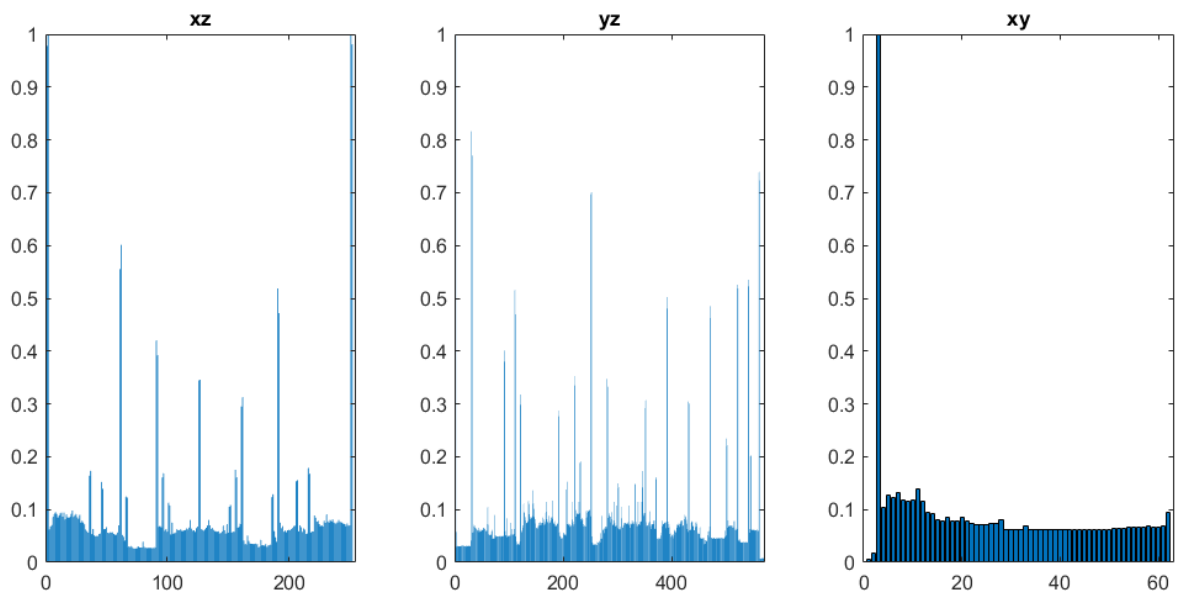


Figure 4.4: Spatial distribution of points in medical camp environment

4.2.3 Forest

The forest environment, considers a cluster of trees to form a dense forest, with very little light penetration from above or side. The GNSS signal reception may be poor in a dense forest. The use of mobile platform in a forest requires navigation through complicated spaces and its intended use can be for survey, inventory purposes and forestry machines require updated tree maps to operate. A good perception system should be able to recognize the

smallest features of obstacle around it in a quick manner. Considering the platform utilizes SLAM as seen in Kukko et al. 2017, and not follow a fixed trajectory, it should have a wide field of view, that allows it to see other possible path options to navigate around the obstacle. Here, the platform follows a fixed trajectory. The trajectory considered here starts from the centre of the forest, having a high density of trees, and moves around the forest, navigating between trees with low-branches. The height considered of the platform here is at $1.5m$ from the ground. The spatial distribution of data can be seen in Fig.4.7. The environment is divided into bins of $10cm$ for each plane (xz , yz and xy). A high density of points is seen in the z direction, xz and yz plane.

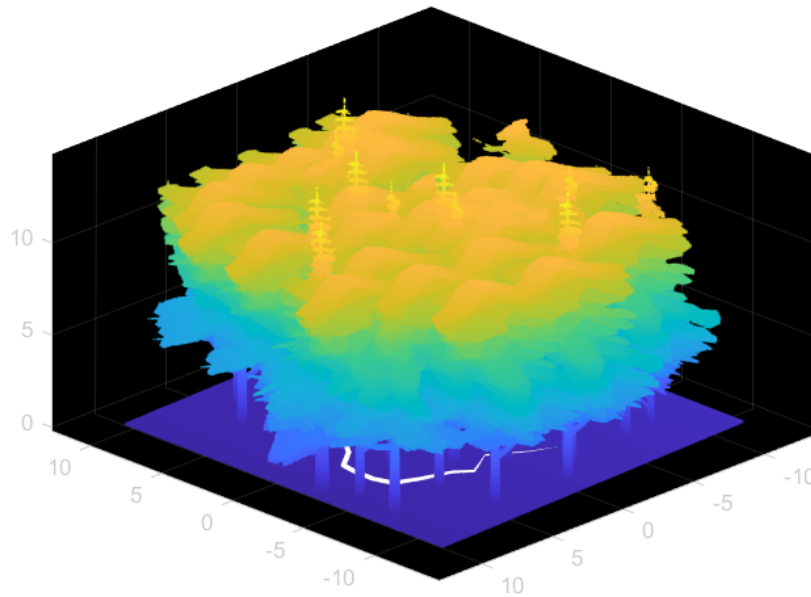


Figure 4.5: Ground truth point cloud of forest environment, displayed with height colouring

4.3 Simulating the Platform

Once the environment is decided, it is required to integrate the chosen LiDAR designs on the mobile platform and begin simulation. This requires certain assumptions and a set up. Costs, mounting designs, and other physical add-ons are not taken into account in the assumptions established for the mobile platform. The mobile platform considered here is $20cm \times 20cm \times 5cm$ in dimension. It is also assumed that the mobile platform has a temporary perception system for navigating the trajectory. The perception system consisting of the proposed LiDAR orientations and configurations is *not* linked to the Navigation module. It is treated as a stand alone perception system that has been used only to capture data. The proposed LiDAR configuration are only mounted on the mobile platform, and the platform follows the trajectory. The data obtained is free of noise and accurate due to the simulation. The data for now, is not utilized for navigation, but can be incorporated in the future. *Velo-dyne Simulator* Inc. n.d. is used for building the perception system. The motion of the plat-

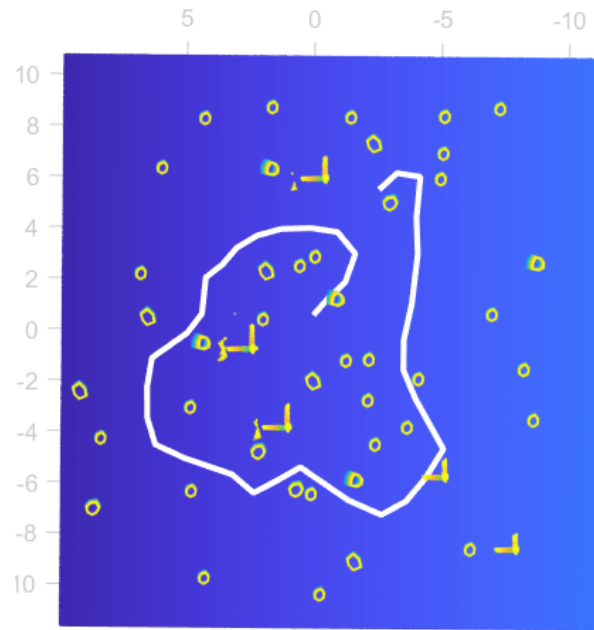


Figure 4.6: Trajectory followed by the platform in the forest environment

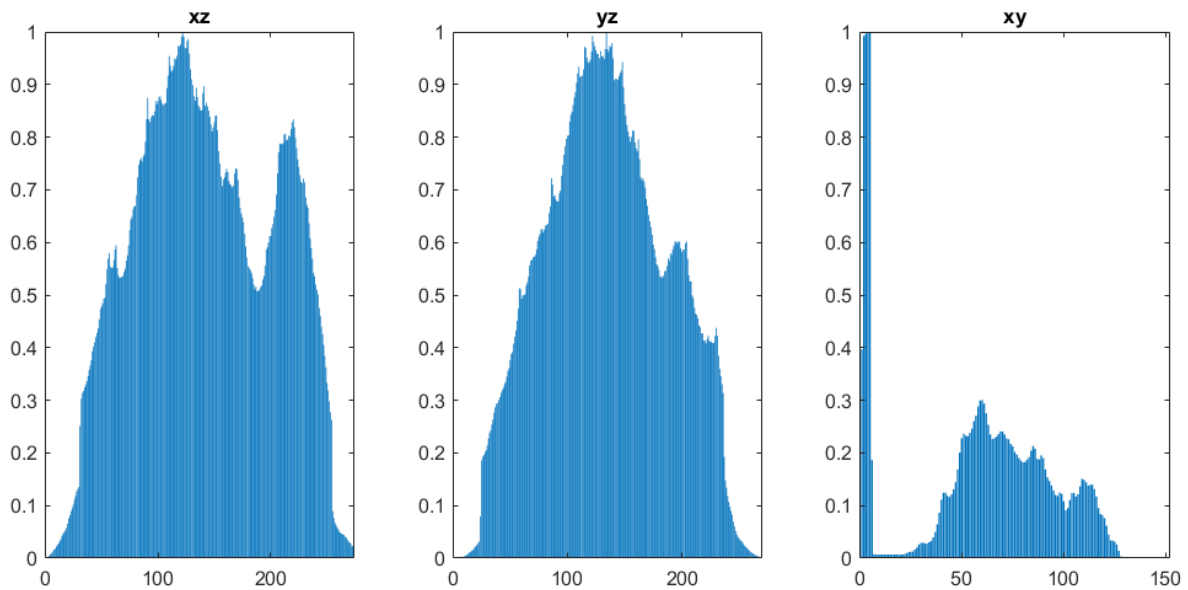


Figure 4.7: Spatial distribution of points in Forest environment

form is limited to 2D so that all configurations are captured under the same circumstances of trajectory. The set up of the mobile platform with the perception system is as follows.

- Produce a map of the environment
- Integrate the LiDAR(s) configuration or the perception system on the mobile mapping platform

- Set up way-points, that build to a trajectory the mobile platform will follow
- Ensure the platform is able to follow the trajectory smoothly and continuously
- Transform the point cloud data from the sensor frame to the fixed world frame

To ensure the platform follows the same trajectory with all the configurations, an expert motion planner is suitable. The *Move Base* is a ROS package that, given a target point in the world, makes an attempt to get there using a mobile base. The package utilizes a *Global* and *Local* planner to ensure the navigation task is completed. The data is gathered in static environments with the local planner being the Dynamic Window Approach (DWA) and the global planner being the Dijkstra's algorithm.

The data obtained from the LiDAR (sensor frame) are transformed to the static world frame and then processed for evaluation. As assumption made is that the navigation system provides perfect data at all times (using a perfect IMU in simulation) and that there is no calibration error between the navigation and perception systems. All designs have the same level of accuracy and precision to study the comparison of various configurations.

Chapter 5

Results

Simulations provide a controlled environment for assessing the quality of the sensor systems. The indoor environments selected for the study are warehouse, medical camp and dense forest. The following chapter is divided according to the environments studied. Under each environment, there is visual analysis of the point cloud followed by the evaluation metric analysis. The environments *Warehouse* and *Medical Camp* have a roof on top during simulation or data capturing. This roof is sectioned out during result analysis, to have a closer, detailed look at the features inside the environment. Hence, there is no roof visible in the figures displayed.

5.1 Warehouse

5.1.1 Visual Analysis

Limited configurations (c1 - c4) are tested in the warehouse environment. The individual configurations are highly dependent on the trajectory traversed. The VLP16 in c1, is oriented such that data can be captured on top (roof) since its scanner axis is parallel to the direction of motion. Unlike in c3, which is mounted on top of the platform, is unable to capture data of the roof. The angular resolution of VLP16, being 2° does leave huge gaps between scans if the point frequency is low as well. Increasing the point frequency decreases this gap, but not entirely as seen in Fig.5.1a. The point cloud captured here is at a point frequency of 900samples . This configuration is unable to capture the vertical dents of the *Europallet* model as seen in Fig.5.2.

There are occluded or shadowed regions visible, which can be reduced by changing the trajectory to cover them. Tilting the LiDAR (VLP16) by 45° reduces the shadows visible during c1, but new regions are included in the blind spot as seen in Fig5.3. The point cloud is recorded at angular frequency of 100 samples . More coverage is observed when the LiDAR is tilted, and the vertical dents in *Europallet* model are slightly better defined.

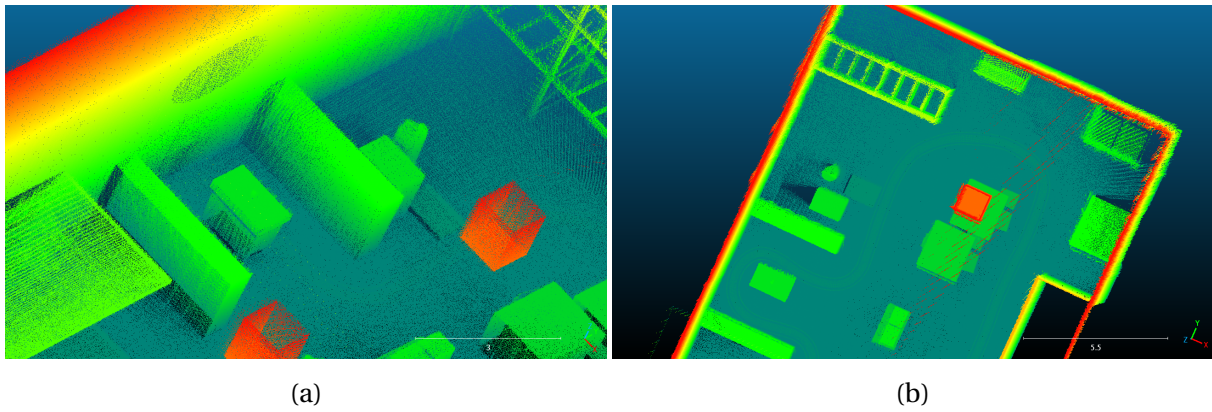


Figure 5.1: Point cloud section of a warehouse as captured from configuration 1 (VLP front)

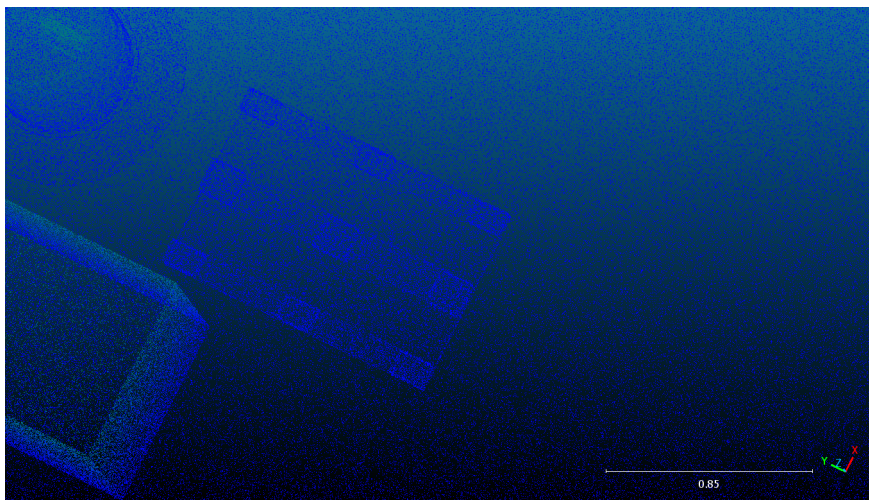


Figure 5.2: Reference point cloud section of *Europallet*

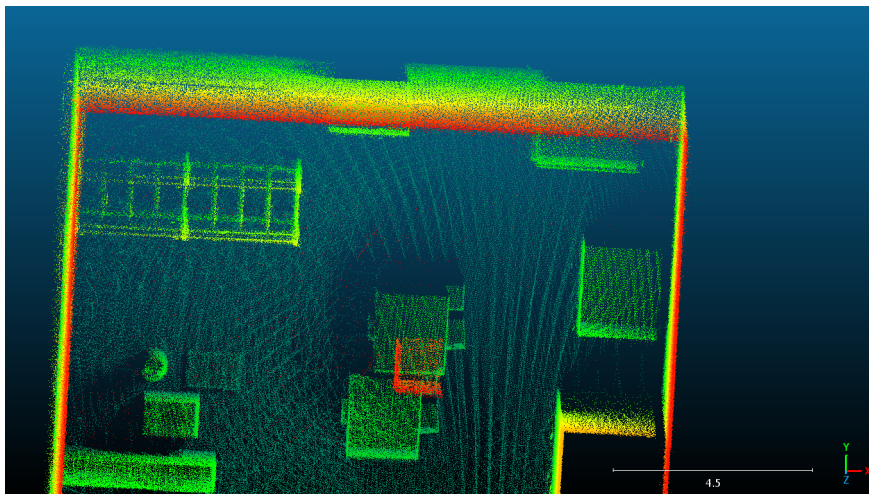


Figure 5.3: Point cloud section of Configuration 2, depiction shadowed regions

Configuration 3, consists of HDL32E mounted on top of the platform. Data is captured in considerable detail on the sidewalls. The point cloud captured with lower sample rate has a better appearance. Data become fuzzier as sample rates are increased. This is shown in Fig.5.4.

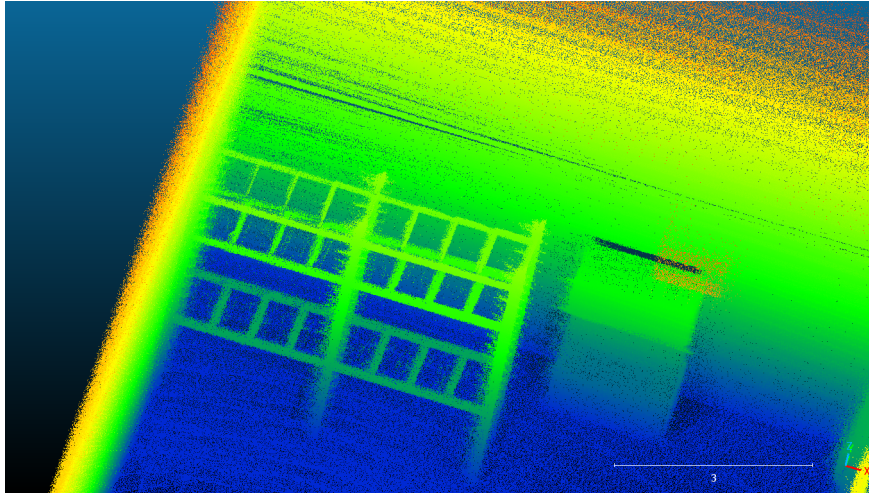


Figure 5.4: Point cloud section of Configuration 3, depiction fuzzy data

Configuration 4, combines HDL32E and VLP16. The point cloud overall looks improved with decreased shadowed regions. Lamp boxes on roof are captured, smaller detail such as the can on the dumpster is visible as well.

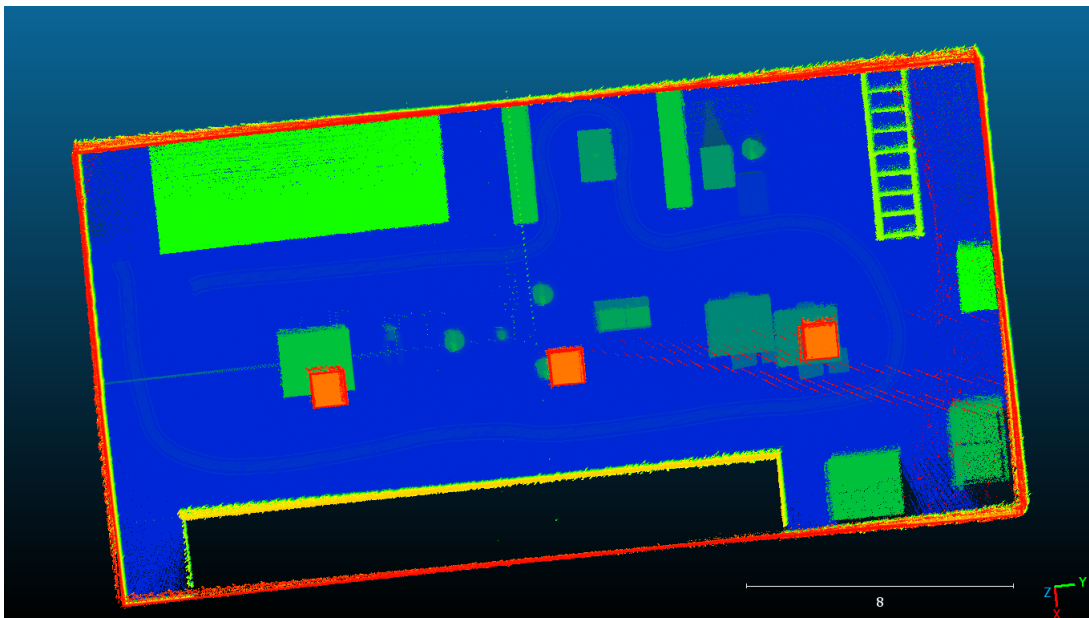


Figure 5.5: Point cloud section recorded by Configuration 4

Configuration	Nominal Point Density	Homogeneity Score	Coverage
1	0.78	0.11	78.2
2	0.77	0.32	82.6
3	0.90	0.2	84.65
4	0.93	0.32	88.3

Table 5.1: Nominal Point density and Homogeneity score for warehouse environment, red highlighting the poor score and green for the best score

5.1.2 Nominal Point Density and Homogeneity Score

The nominal point density (NPD) value is highest for c4, followed by c3. This can be due to the high number of lasers (HDL32) used in both the configurations, which contribute directly to an increasing score of NPD. The lowest value is for c2, but it also shows the highest homogeneity score. C2 configurations visually shows more occlusions than the other configurations, this reduced the NPD value. But because of the inclined scan-lines, which form an overlapped pattern the homogeneity score increases.

5.1.3 Coverage

The coverage for warehouse environment is calculated by setting the *cut-off* distance at $0.5m$. A detailed analysis of the *cut-off distance*, and *coverage* is seen for the next environment 5.2.3.

Insight:

The warehouse simulation is of small environment, which does not provide much intuitive analysis scenarios. The point clouds obtained are comparable with a standstill LiDAR platform placed at the center of the environment. *Tier 1*, c3 is a good set-up for an environment such as a warehouse. It obtains a good coverage, with an average NPD value. Although c3 has a more expensive, power consuming and heavy LiDAR compared to other configurations, it should be understood that a similar LiDAR, with similar specifications can be utilized, such as VLP32.

5.2 Medical Camp

5.2.1 Visual Inspection

Configuration 1 and 2 depict different scan patterns as seen in Fig5.6b. Tilting the LiDAR at an angle, provides more closer scan lines, or reduced point spacing, refer Fig5.7b.

In config3, the bottom of the room is not scanned, though it is part of the trajectory. Scan

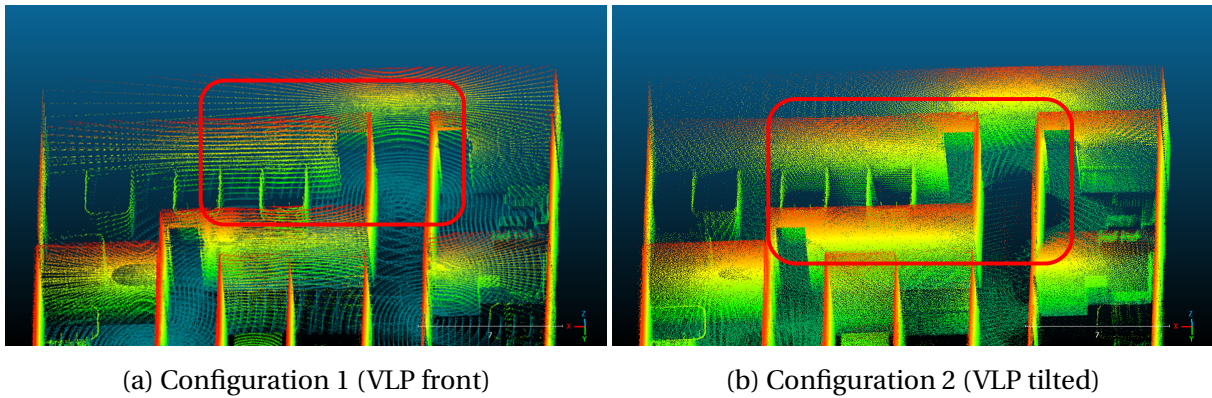
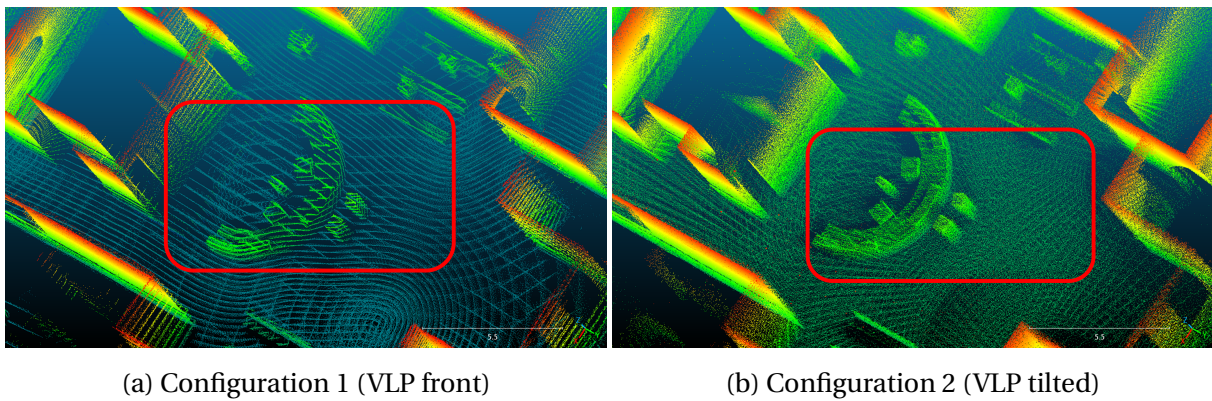


Figure 5.6: Point cloud section of scan pattern seen for VLP16 LiDAR

Figure 5.7: Point cloud section of *Reception* model seen for VLP16 LiDAR

lines are restricted to the FoV and the room dimensions are smaller for the laser beam to reach the floor.

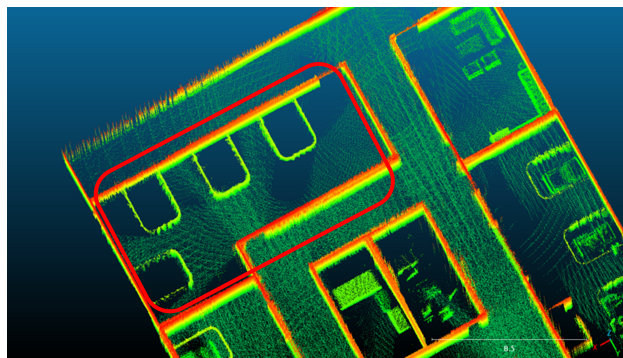


Figure 5.8: Point cloud section of a room in hospital captured from configuration 3

Fig.5.9 displays a section of the medical room not spanned by the mobile platform. Adding the Velarray fictional LiDAR increases the visibility range. The *patient bed* which were not scanned earlier with config1 are now visible in config5.

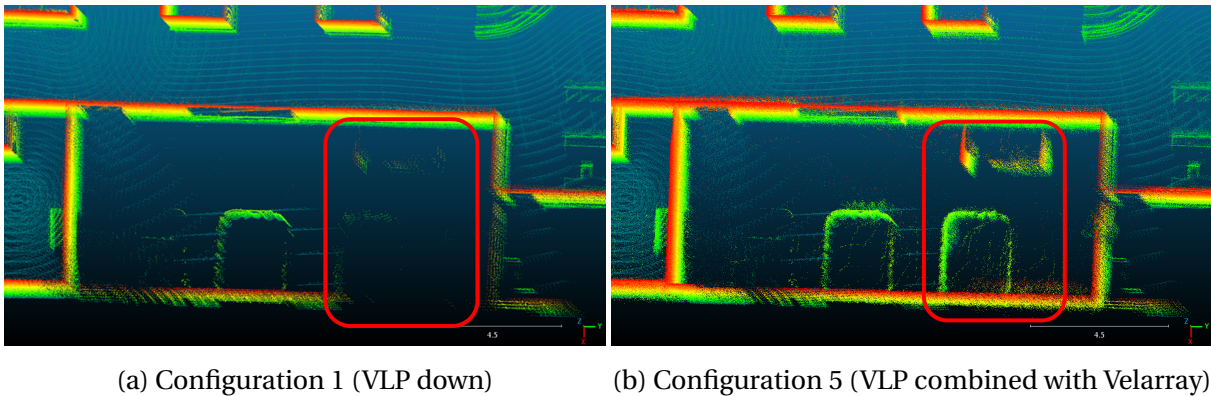


Figure 5.9: Difference in point cloud recorded by configuration 1 and 5

Between configuration 2 and 6, the shadowed region is reduced as seen in Fig.5.10.

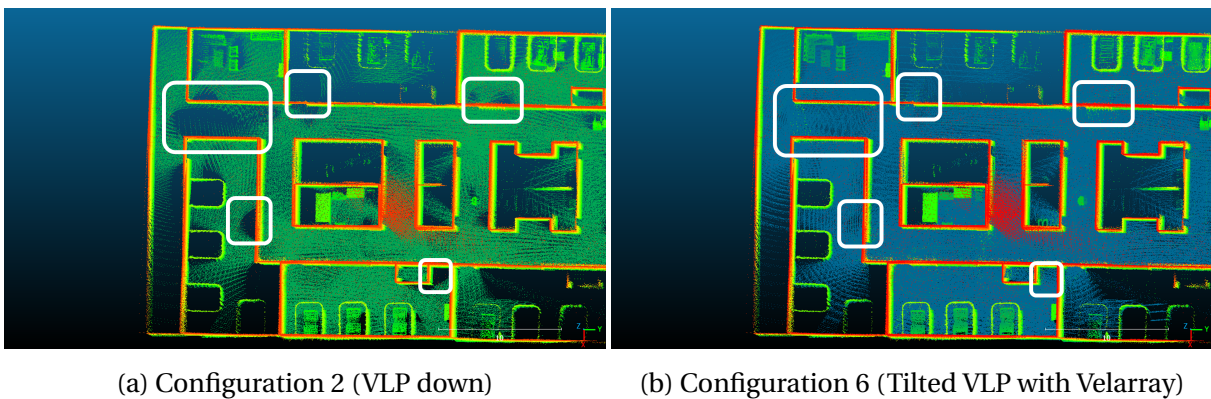


Figure 5.10: Difference in shadowed region from point cloud recorded by configuration 2 and 6

Configuration 4,5 and 6 belonging to *Tier 2*, consists of two LiDAR for scanning. The three configurations have their own advantages, and scan the environment to similar detail. But it is interesting to observe the corridor, which does not get traversed by the mobile platform is scanned to a certain extent by config4 (Fig.5.11). It is scanned well by config5 (Fig.5.12) and but only partially by config6 (Fig.5.13).

Configuration 8, combines all three LiDAR. The point cloud (Fig.5.14) obtained, contains very minimal occlusions but excessive data. This configuration can be applicable in scenarios where high density of point cloud is required. It is able to capture the smallest detail of the room in one sweep of the mobile platform.

Configuration 7 consists of three LiDARs as well, performs very similar to c8. Except it is unable to scan the roof as well as c8. Only sparse data is visible for roof.

Configuration9 is tested out in hopes it can be a possible replacement for the common 360°

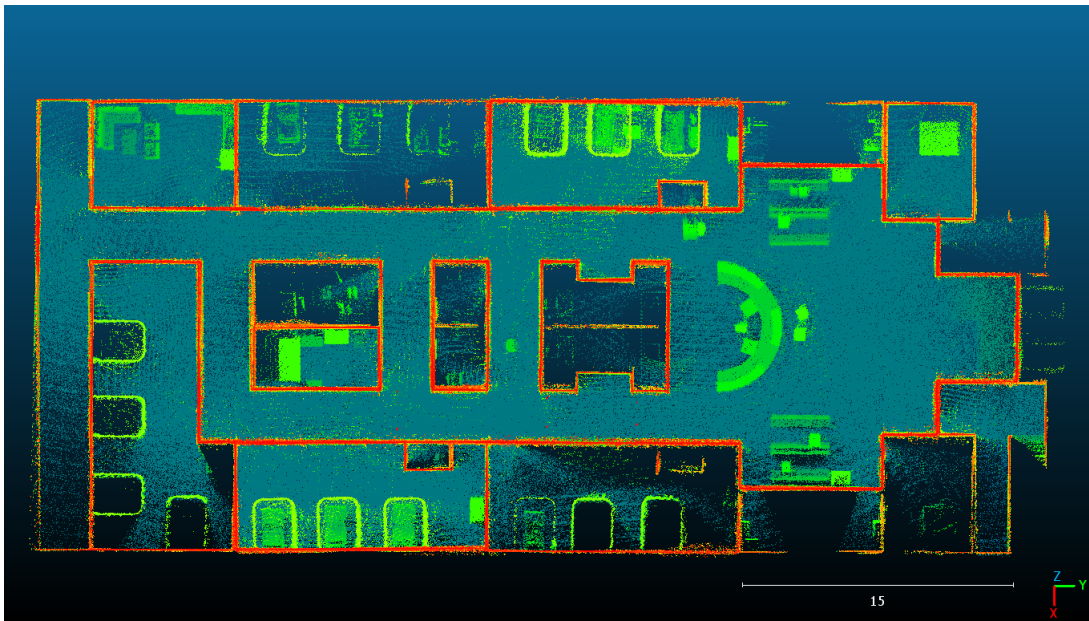
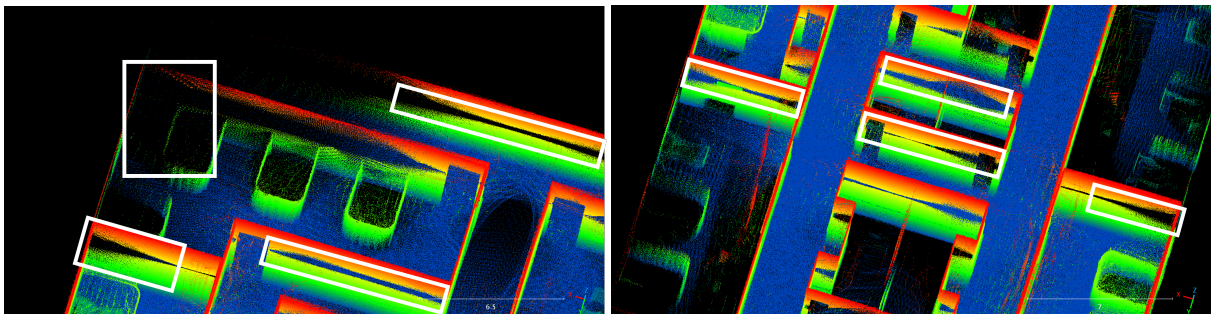


Figure 5.14: Point cloud simulated from configuration 8

LiDAR, this can be improved by either increasing the VFoV or reducing the tilt angle of the LiDARs, such that there is an overlap in the scan lines. This will come at an additional cost of not being able to scan the roof as it does now.



(a) Corridor at the back not scanned with configuration 9

(b) The walls have a gap in the middle where scanning points are not visible

Figure 5.15: Point cloud simulated from Configuration 9

Summarizing the visual inspection observed, in a Tabular format in Table 5.2

Table 5.2: Visual Analysis for medical camp environment

Configuration	Remarks (Visual)
C1	Roof visibility ✓ Sparse scan lines, requires high sample points for coverage
C2	Roof visibility ✓✓ Scan pattern provides better coverage (compared to c1) Shadowed regions increased
C3	Roof visibility × Unable to scan floor in narrow regions More lasers → dense point cloud produced
C4	Roof visibility ✓ Occlusions observed in c3 are reduced here Spaces without a trajectory such as corridor scanned
C5	Roof visibility ✓ Additional features from a room not scanned visible Most features scanned in detail
C6	Roof visibility ✓✓ Shadows visible during c2, reduced Most features scanned in detail
C7	Roof visibility × Dense point cloud Features scanned in detail
C8	Roof visibility ✓ Point cloud very similar to c7
C9	Roof visibility ✓ Contains regions in the middle without any scan points Unable to scan features in detail

5.2.2 Nominal Point Density and Homogeneity Score

The reference point cloud considered has a mean point density, ρ_D of 1million pts/m^3 . The mean point density calculated, is used as a measure of how dense a point cloud is obtained with combinations of LiDARs. It was expected configuration 7 or 8 to have the highest point density, given it is a 3 LiDAR configuration. Comparing the configurations according to the *Tiers* they are divided in provides a better analysis.

Tier 1 consists of single LiDAR of 16 and 32 lasers. Increase in number of lasers increases the nominal point density of the point cloud as seen for Configuration 3. But this does not translate to a more homogeneous point cloud. Configuration 1 and 2, have approximately similar point cloud density but a slight tilt in the orientation of the scanner results in an expected increase in homogeneity score. This can be understood, as the profile spacing reduces. But excessive tilt will also degrade the quality of point cloud. This is further explored in section 5.2.4.

Tier 2 consists of two LiDAR scanner. It is interesting to observe the configurations (4,5, 6) have a similar nominal point density, but c6 has the highest homogeneity score. In case of this, it is useful to look at the profile spacing or scan lines. Although the higher score can also be due to the orientation of the additional flash LiDAR in downward direction, which improves c2.

Tier 3 consists of three LiDAR scanners. The homogeneity score of c9 is the lowest, which is also confirmed from visual analysis. The horizontal gap seen from the point cloud obtained with c9. The nominal point density is highest for c8, followed by c7. c7 also has the second highest homogeneity score.

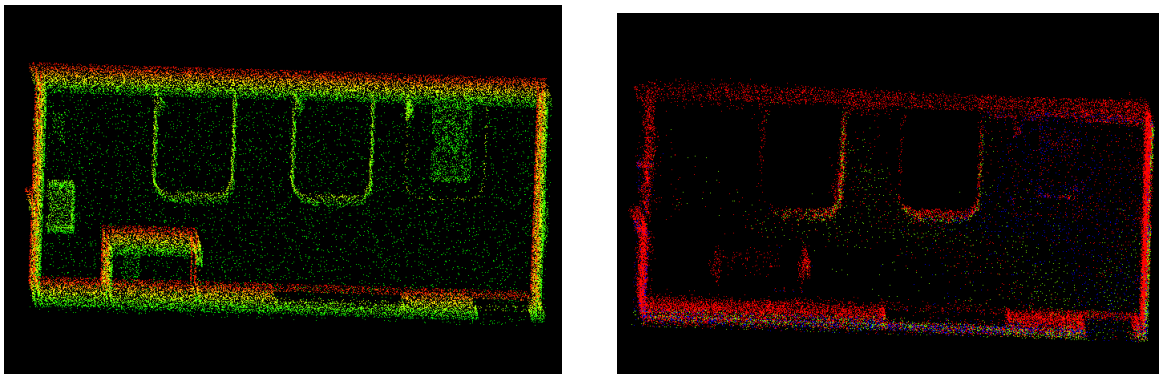
5.2.3 Coverage

The coverage is calculated with reference to the original point cloud build using collision models from the environment. Due to the complexity and limitations of the processing capability of the laptop, the simulated point cloud is down-sampled. The down-sampling is done using the '*random subsample*' feature of *CloudCompare*. This ensures the point cloud coverage is not effected non-linearly. The homogeneity and density are not considered during the calculations. Coverage provides an estimate of how much part of the original point cloud is covered by the simulated point cloud. The *cut-off* distance considered between the two point cloud is $0.3m$. This has been calculated by carefully assessing the trend with which the coverage varies with cut-off distance. A section of the the medical camp point cloud is considered as seen in Fig.5.16. The coverage saturates after a certain cut-off distance as seen in Fig.5.17. The cut-off distance is calculated by drawing the tangent at point of inflection,

Configuration	Nominal Point Density	Homogeneity Score
1	0.68	0.188
2	0.72	0.209
3	0.787	0.183
4	0.805	0.190
5	0.801	0.198
6	0.805	0.36
7	0.812	0.256
8	0.815	0.217
9	0.782	0.168

Table 5.3: Nominal Point density and Homogeneity score for medical camp environment, red highlighting the poor score and green for the best score

thereby determining the cut-off distance as $0.3m$. For visualization of *coverage* the reference point cloud is coloured blue for points scanned, and in yellow for not scanned points as seen in Fig.5.18.



(a) Section of original point cloud used to calculate coverage cut-off (b) Section of simulated point cloud to calculate coverage cut-off

Figure 5.16: Point cloud section used to calculate cut-off distance

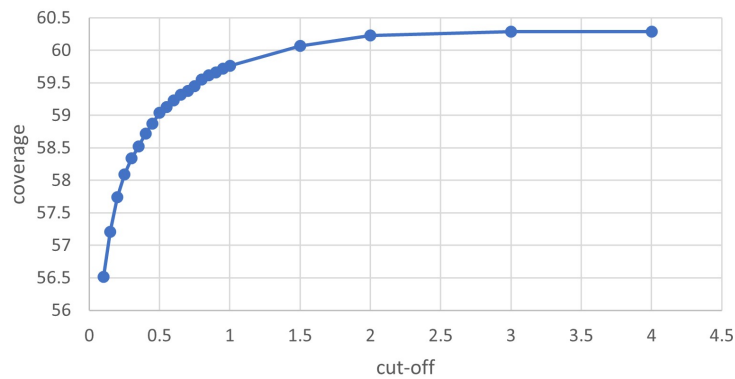


Figure 5.17: Graph of Coverage vs cutoff distance

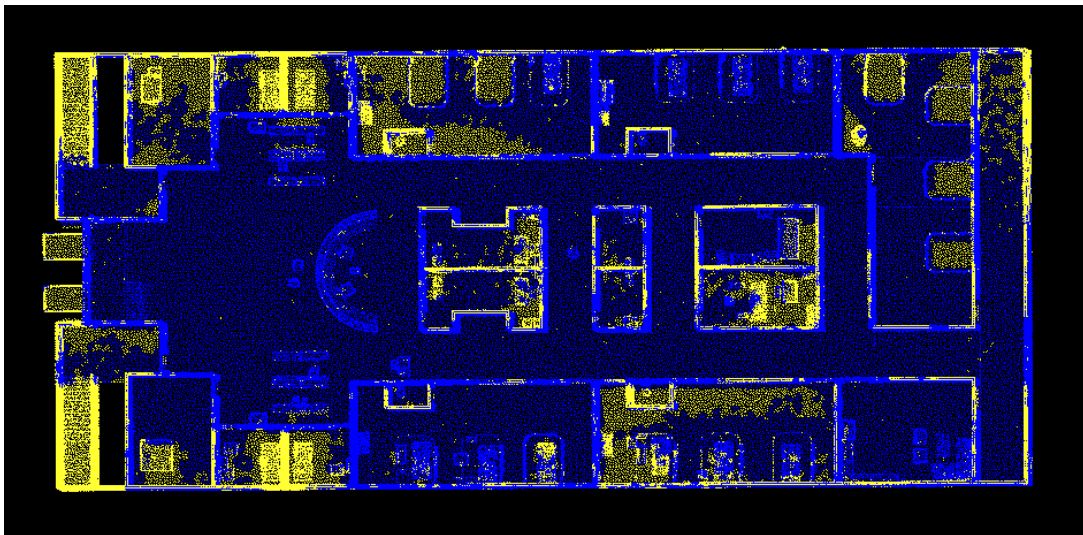


Figure 5.18: Coverage point cloud for Configuration 7, Yellow points are unscanned regions, and Blue points are scanned regions

With the configurations considered for medical camp environment, it is expected Tier 3, c8 will have the highest configuration, with the LiDAR placement. This is observed in Fig.5.19. Configuration 8 has the highest coverage of 82.91%, followed by configuration 4 with 82.42%. The increase in number of LiDAR from c8 to c4 does not make a huge difference in coverage. The next best configuration is c7, with 77.22% coverage. The least effective configuration is c9, providing 69.52%.

Insight:

Overall, for an environment such as a medical camp, even though c8 provides the highest coverage, c7 could be a smarter alternative. C7 provides visually similar point cloud as c8, except for roof not covered, and a good nominal point cloud density and homogeneity score.

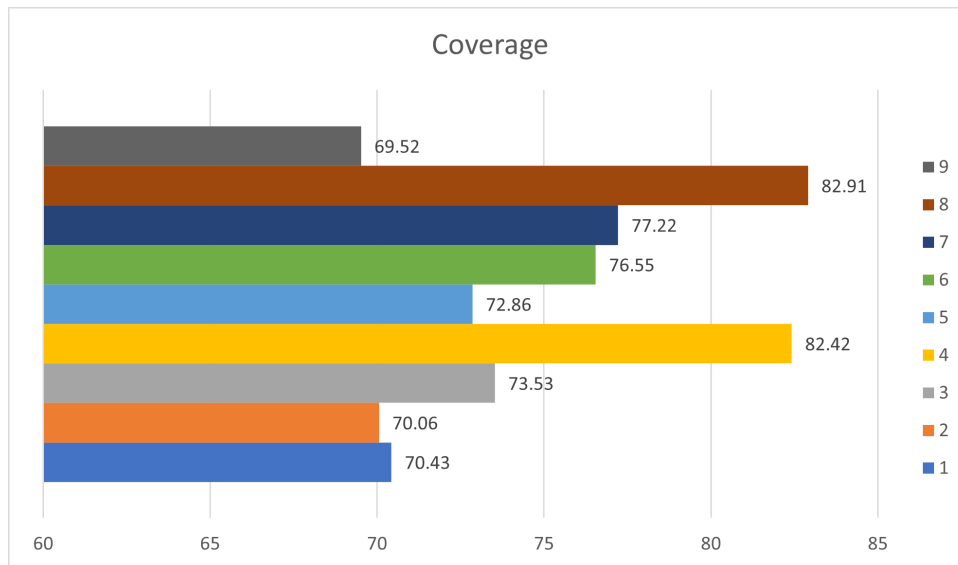


Figure 5.19: Point cloud coverage for each configuration in the medical camp environment

Both configurations 7 and 8 consists of three LiDARs. But in comparison to c8, c7 has two simulated flash LiDAR and one scanning LiDAR. Flash LiDAR weigh lesser, and are more affordable when compared to scanning LiDAR and have lesser power consumption. An optimal configuration for each Tier can be observed. *Tier 1*, a combination of c2 and c3 would be ideal. Adapting the orientation of c2 and increase in number of lasers from c3. In *Tier 2*, consisting of two LiDARs, for high coverage c4 is good, but for higher homogeneity score c6 is a better choice. *Tier 3*, as discussed before between c7 and c8, c7 is a preferred choice.

5.2.4 Range and Orientation of LiDAR

The previous scenarios show the significance of tilting the orientation of LiDAR to increase the quality of point cloud obtained. Inclining the sensor has a high advantage, as explored in Samer Karam et al. 2019. To understand the influence of the inclination angle on the quality of point cloud, the medical camp environment was considered, with the same trajectory. Using only *VLP – 16* as the LiDAR, with increment of 15° in the inclination, the point cloud obtained were assessed. Table.5.5 summarizes the results of change in inclination angle. The NPD (Nominal Point Density) gradually increases with the decrease in inclination angle, from 90° to 0° . The coverage does not significantly decrease from 90° to 30° , the change is 0.83%. The decrease from 30° to 15° is 3.17% compared to decrease from 15° to 0° of 5.33%. The optimal orientation is at 45° with a good NPD and coverage. The penalty of inclining the LiDAR comes with occlusions or shadows present in the point cloud.

Table5.4 shows the influence of the range of the LiDAR on coverage. The Flash LiDAR have shorter range of 30-40m when compared to the scanning LiDAR of 80-100m. The change in coverage from 20m to 40m is 4.05%, but coverage from 60m to 100m is only 0.42%. With a

mobile platform, a mid-range sensor performs good.

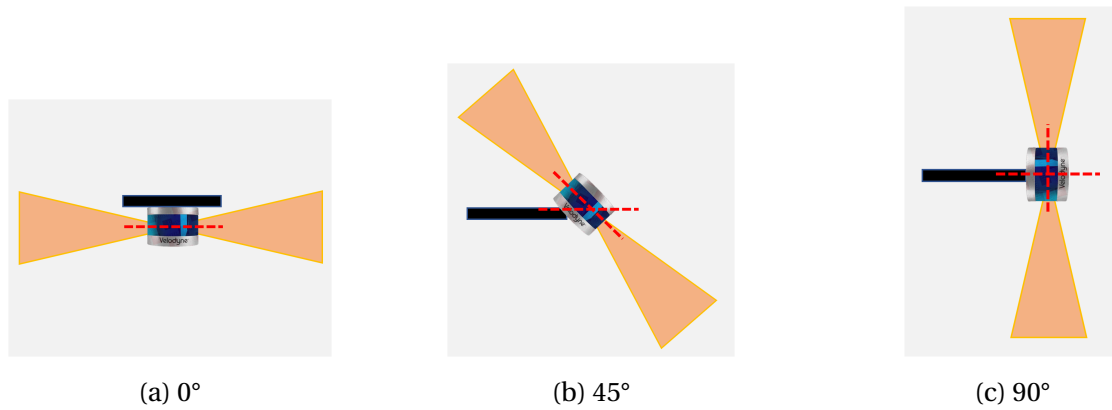


Figure 5.20: Single LiDAR mounted on a small mobile platform with changing orientation

Range	20	40	60	80	100
Coverage	68.3	73.05	74.06	74.42	74.48

Table 5.4: Coverage calculated for different range of LiDAR

Inclination Angle °	Nominal Point Density ρ_D	Coverage
90	0.68	70.42
75	0.67	69.47
60	0.69	69.63
45	0.72	69.77
30	0.73	69.59
15	0.74	66.42
0	0.75	61.09

Table 5.5: Nominal point density and Coverage for change in inclination of a single LiDAR (VLP16) in medical camp environment

5.3 Forest

5.3.1 Visual Analysis

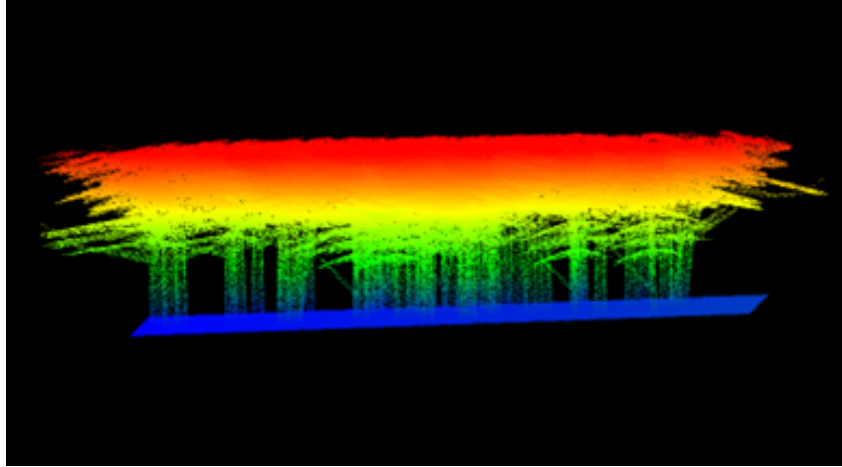


Figure 5.21: Section of forest point cloud, considered for reference

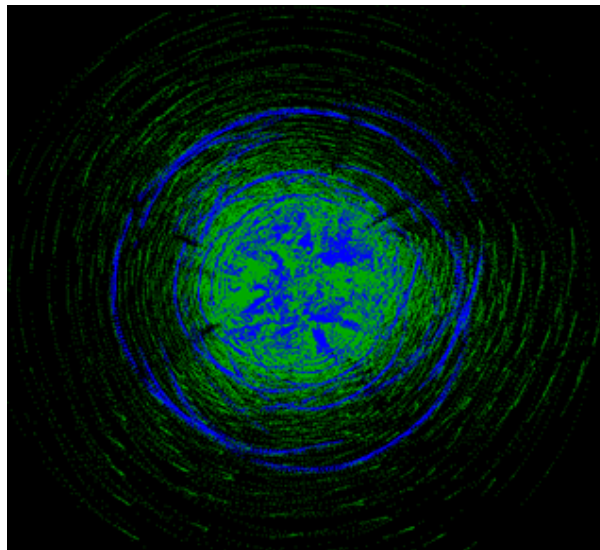


Figure 5.22: Comparison of top view of point cloud as seen from c1 (blue) and c2 (green)

The forest environment, is spatially distributed in the z -direction. The top half portion of the trees are not visible to the LiDAR, because of the dense canopy of trees present which simulates it as an indoor environment. Only a section of the forest point cloud as seen in Fig.5.21, is considered for reference. This is the portion assumed to be visible to the LiDAR, and the laser pulses can not penetrate higher than this section.

Configuration 1, shows fuzzy coverage of the point cloud as seen in Fig.5.23. The tree trunks have sparse coverage, which can be increased by increasing the point frequency of LiDAR. There is light visibility of leaves above the dense canopy section.

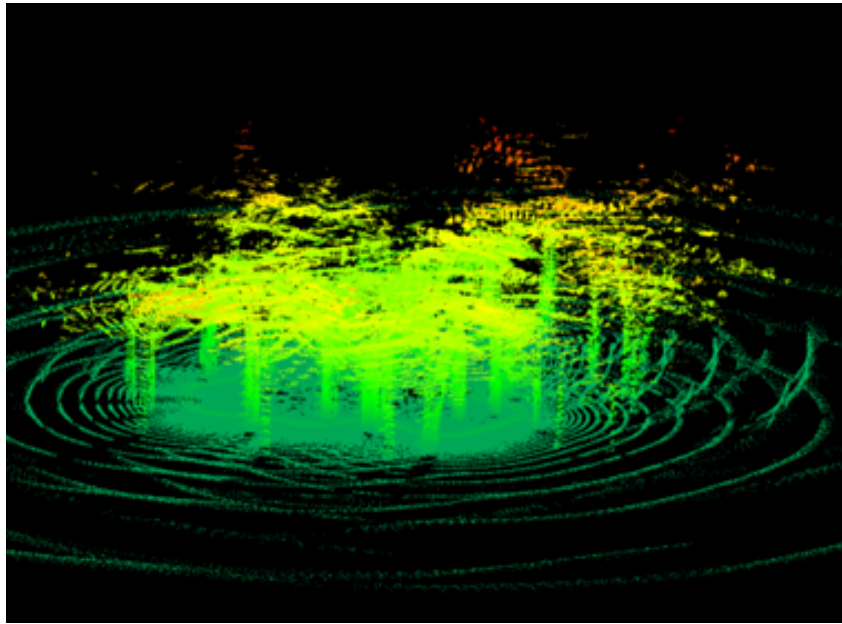


Figure 5.23: Point cloud obtained from configuration 1

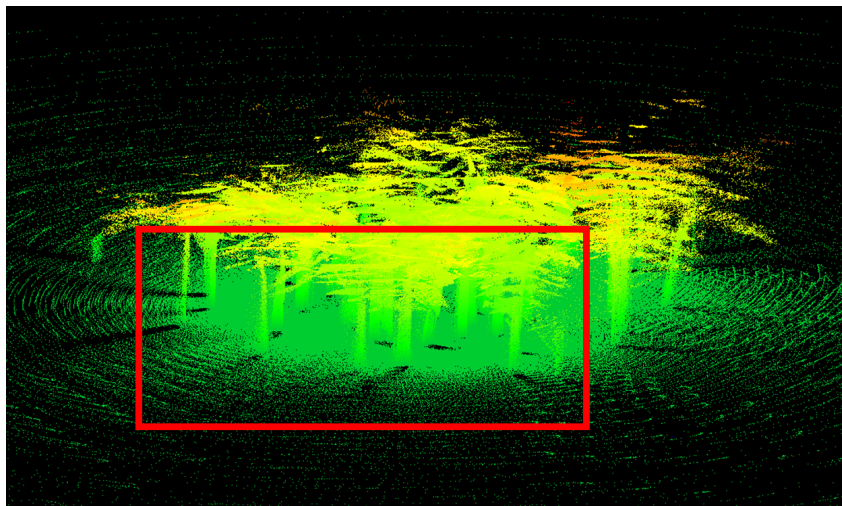


Figure 5.24: Point cloud obtained from configuration 2

Configuration 2, clearly has a denser point cloud generated compared with configuration 1, at the same point frequency. The tree barks as seen in Fig.5.24 are clearly visible now. There is a similar light visibility of leaves from before. Due to the tilt in configuration, there are shadowed regions visible around the tree barks. The range of visibility between configuration 1 and 2 (c1 c2) is seen if Fig.5.25. c2 has a longer range of visibility.

Configuration 3 & 7, have a poor visualization of point cloud. As seen in from Fig5.25, c3 does not capture the dense coverage of canopy, it is only able to visualise the tree barks. Fig.5.28, shows a slight improvement in capturing the tree barks batter. But no overall im-

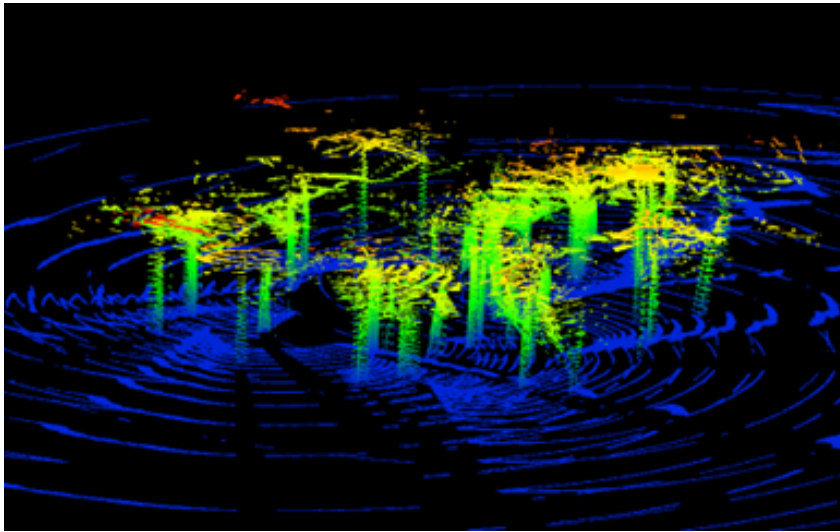


Figure 5.25: Point cloud obtained from configuration 3

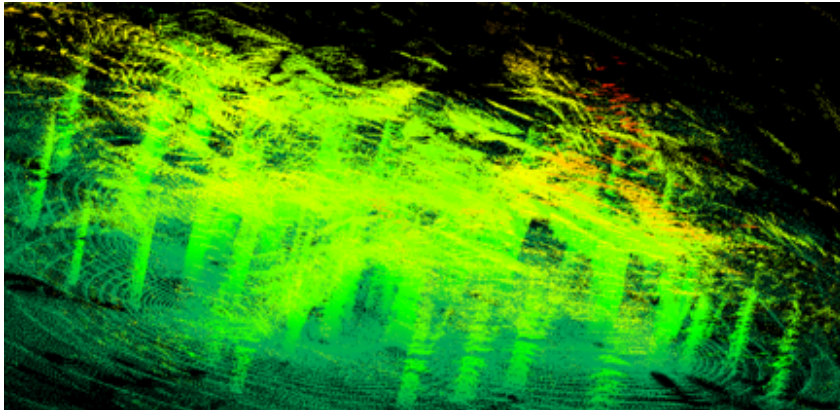


Figure 5.26: Point cloud obtained from configuration 5

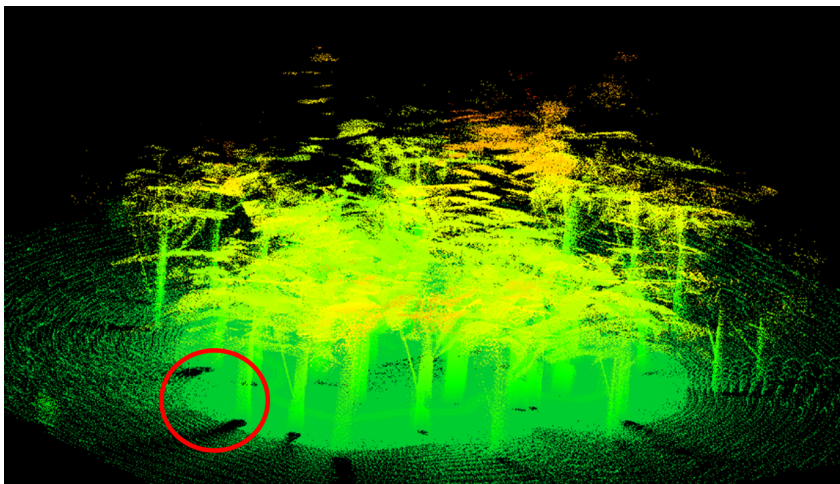


Figure 5.27: Point cloud obtained from configuration 6

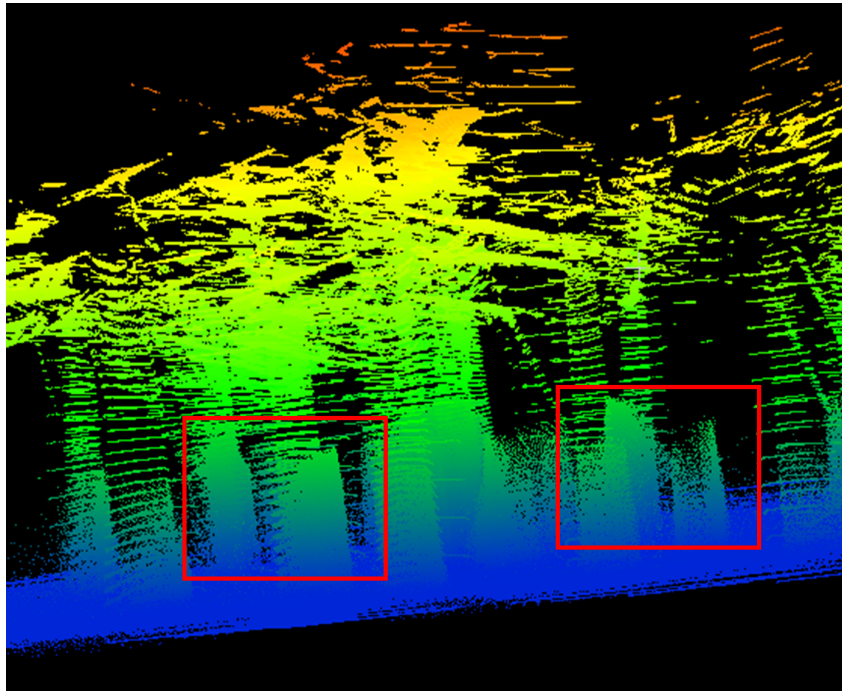
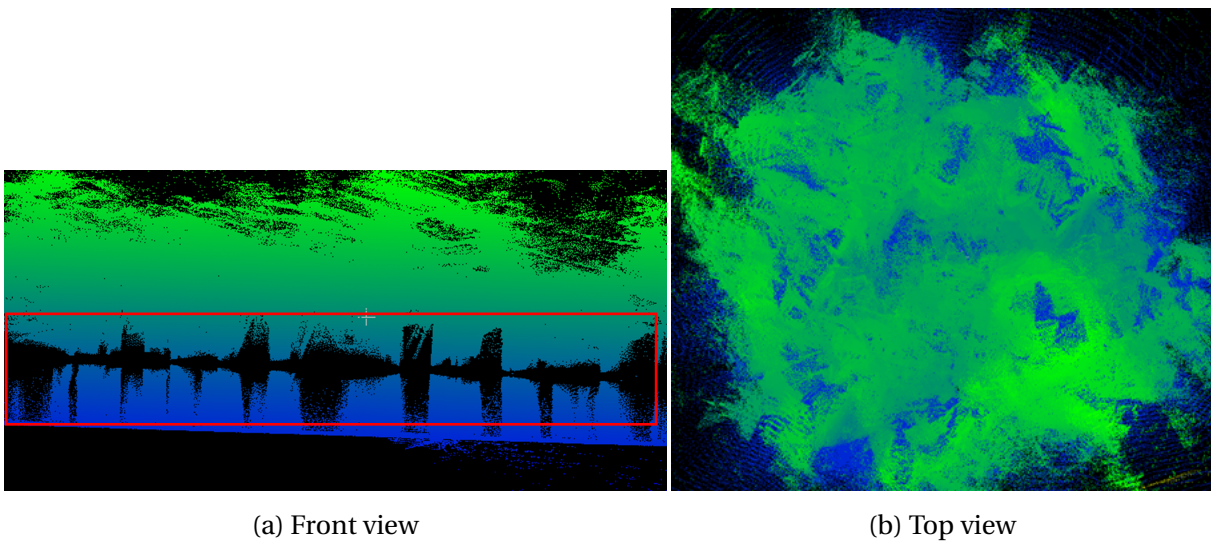


Figure 5.28: Point cloud obtained from configuration 7



(a) Front view

(b) Top view

Figure 5.29: Point cloud obtained from configuration 9

provement seen in the recorded point cloud.

The sparse tree barks seen with c1, are reduced in c5 (Fig.5.28, especially towards the inside of the canopy). In a similar manner, c8 is an improvement on c2. As seen in Fig.5.27, The shadows around the trees have reduced. A few occlusions are still visible on the outer rim, which can be reduced with the change in trajectory.

Configuration 9 gives an overall better coverage of the canopy leaves on top, seen in Fig.5.29b. But due to the orientation of the LiDARs, there is a gap visible (Fig.5.29a) in the point cloud, with no points. Changing the LiDAR orientation to overlap their FoV, or increasing their FoV will reduce this gap.

Summarizing the visual inspection observed, in a Tabular format in Table 5.6

Table 5.6: Visual Analysis for forest environment

Configuration	Remarks (Visual)
C1	Range of visibility from LiDAR lesser compared to c2 Fuzzy coverage of the sectioned forest Sparse visibility of leaves above the dense canopy
C2	Denser point cloud generated Clear visibility of tree barks Similar coverage of leaves as seen in c1 Shadow of tree trunks visible (occluded regions)
C3	Poor visibility of point cloud The dense canopy not seen at all
C4	No additional features seen compared to C1 Point cloud same as of c1
C5	Fuzzy branches as seen in c1 Fuzziness reduced towards the inside of canopy
C6	Occlusions of the tree barks seen in c2 reduced towards the inner part of canopy A few occlusions still visible on the outer rim
C7	Visibility of the bottom half of tree bark a little better to c3 Not much of an improvement to c3
C8	Improvement in the visibility of tree barks No gaps as seen in c9
C9	Gap in point cloud in the middle Overall a better coverage of the canopy (leaves) on top

5.3.2 Nominal Point Density and Homogeneity Score

The reference point cloud considered has a mean point density, ρ_D of $10^4 \text{ pts}/m^3$. The mobile platform is at a height of $1.5m$ in this environment. With the height of the platform (on which the sensors are mounted) is reduced, the nominal point density and homogeneity score is increased overall.

In *Tier 1*, both the best and worst homogeneity scores are observed by c2 and c3 respectively. Even though c2 has the highest homogeneity score, it also has the overall lowest NPD. But when compared to the NPD value of other configurations in *Tier 1*, the value is for c2, is reasonable. The low homogeneity score of c3 goes along with the poor visualization of the point cloud, from previous section.

Tier 2, displays same homogeneity scores for all configurations and an average NPD value. *Tier 3*, is more interesting to analyze. c7, which has a poor visualization, also has the highest NPD value, and second highest homogeneity score. The NPD is dependent on the number of points within a particular area (sphere), and with more laser pulses striking the surface, the NPD will tend to increase. But this does not translate to better coverage directly, since the increased laser pulses are restricted according to the FoV and orientation of the scanner, they can only strike against a portion of the environment. The high homogeneity score of c7 is due to the points covering the floor portion. Calculating the homogeneity score without the floor included, reduces the score to 0.22, making it the overall lowest score then.

Configuration	Nominal Point Density	Homogeneity Score
1	0.83	0.42
2	0.81	0.43
3	0.89	0.28
4	0.91	0.35
5	0.84	0.35
6	0.91	0.36
7	0.98	0.42
8	0.95	0.39
9	0.94	0.41

Table 5.7: Nominal Point density and Homogeneity score for forest environment, red highlighting the poor score and green for the best score

5.3.3 Coverage

The coverage for the forest is calculated by setting the *cut-off* distance to $0.3m$. Fig.5.30 shows the coverage chart for this environment. Configuration that was previously ideal for

the medical camp is now exhibiting inadequate coverage. The highest coverage of 59.64% is seen from c9.

Insight:

Config9 can be a good replacement for the 360° scanner. The gaps observed by c9 during visual analysis, can be eliminated by changing the inclination of the LiDAR, such that the FoV are overlapping. The next best configuration is c4 and c5, both containing the flash LiDAR. Configuration c3 and c7 have the lowest coverage of 41.57% and 45.73%.

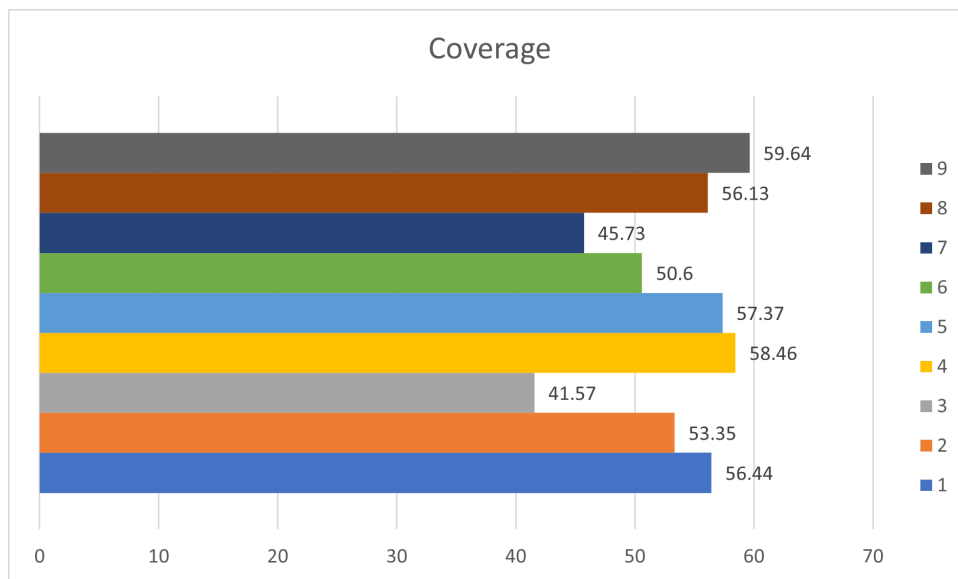


Figure 5.30: Point cloud coverage for each configuration in the forest environment

Chapter 6

Discussion

6.1 Discussion

Three Environments with nine design configurations inspired from state-of-the-art mobile platforms were simulated. The complexity of the problem increased with the variables considered necessary for analysis. In the environment, it was necessary to have a fixed trajectory to follow. To reduce the complexity, the mobile platform was restricted to 2D navigation (in the xy plane). LiDAR specifications such as point frequency (sample points), field of view (FoV), range, number of LiDARs, orientations of LiDARs and number of laser beams were varied as control parameters. It was determined that these variables effect the point density of the point cloud. The point density is linearly dependent on point frequency, and hence it was kept as a fixed variable in all scenarios.

To gain an insight into the overall performance of the point cloud quality, for various configuration under different environments, we compare the results of individual point clouds across an evaluation metric. The evaluation metric consists of the *Nominal Point Density*, *Homogeneity Score* and *Coverage*. The scores are calculated against a reference point cloud build from the collision of the models in the environment. The environments considered are restricted to be indoor, static environments with an application of a small mobile mapping system. The *warehouse* and *medical camp* are organized environments, with a defined pathway, rooms and structured, rigid models. The *forest* is an *unorganized* environment consisting of trees of different shape and height. Between the two organized environments, the warehouse environment is smaller with the dimensions of $7m \times 5m$, compared to that of a medical camp with $25m \times 57m$ in dimension. The point cloud recorded with the small environment are not sufficient for the analysis, it is more inclined to be compared with a standstill LiDAR placed at a convenient center of the environment.



Figure 6.1: Summary from evaluation metric

Fig.6.1 shows a cumulative result of the evaluation metric. The length of each bar represents the value of NPD, homogeneity and coverage for every configuration. As it can be seen, the lowest score of NPD belongs to *Tier 1*, specifically c2 (warehouse and forest) and c1 (medical camp). And the highest NPD score belongs to *Tier 3*, c7 (forest) and c8 (medical camp). A NPD score can only be understood as the point density in the cloud for a given constant point frequency. The NPD is influenced by different factors, such as, the height at which the platform is capturing the data, the number of laser beams used in the LiDAR, the velocity of the mobile platform and the number and orientation of the LiDARs. In medical camp environment, the mobile platform is at a height $3.4m$, compared to the forest environment, the mobile platform is at a height of $1.5m$. The range of NPD is seen higher for the forest environment, but this is also because of the dense, closed canopy created by the trees. The medical camp in comparison, is a little more spacious, and the mobile platform has more space around it, it does not fly close to the objects to capture the data. Another important factor is the number of lasers in the LiDAR. Increasing the number of lasers and number of LiDARs increases the NPD value. A high NPD value is required for better visualization of smaller details.

The homogeneity score, provides us insight of the uniformity of the points in the point cloud. It is accepted that the recorded data will not be uniformly captured, but to what extend this non-uniformity is present? Highly non-uniform data also results in misinformation. For the different environments present, different configurations record the best and worst scores for homogeneity. This score is dependent on the orientation of the LiDAR. Warehouse environment, depicts tilting of the LiDAR (c2) provides a better score than c1. In the medical camp, it is interesting to observe c6 provides the highest score. C6, is an improvement on c2. The lowest score for medical camp is recorded for c9, this can be improved by changing the orientation of the LiDARs. The lowest score in forest environment is by c3, even though the LiDAR has 32 laser beam, due to its orientation and FoV, it is unable to capture the details of the environment.

Coverage provides information on the geometric visibility of the point cloud as recorded by each configurations. The coverage is sensitive to the cut-off distance. A large cut-off distance puts additional weight on the outliers, and a smaller cut-off distance is unable to capture significant details. Overall some configurations perform than the others in terms of coverage, but that can not be the only choosing factor. The highest coverage, might not be the optimal choice always, but definitely provides a benchmark or a similar alternative. The optimal configuration chosen for medical camp does not have the highest coverage, but is a balance between all the evaluation criteria and the cost/design factor. In the forest environment, c9, provides the highest coverage and is suggested as a good alternative to the traditional configurations.

The range and the orientation of the LiDAR influence the coverage obtained directly. It is

observed that mid-range sensors perform well on a mobile mapping platform. The orientation is crucial. Inclining the LiDAR increases the coverage, but also increases the shadowed regions. An inclination of 45° was seen optimal according to the evaluation metric.

The visualization table presented for medical camp and forest environment, on most cases supported the analysis obtained in accordance with the evaluation metric. But there are occasional exception cases, such as *forest* environment, c7 configuration. This configuration displayed poor visualization of the point cloud, with no features clearly visible, but still has the highest NPD and homogeneity score. This was because of the orientation of LiDAR, which collected high amount of points from the floor portion. The coverage of c7 was poor supporting the visualization. The evaluation metric developed here, can not be used as a standalone factor. Visualization needs to act as a qualitative assessment of the point cloud quality as well.

Overall, the type of LiDAR used by a small mobile platform is determined by a combination of factors, including the platform's design, its intended application, and the availability and performance of LiDAR technology. The research done here shows the viability of incorporating additional LiDARs for different intended use and application. But this raises the questions of how many LiDARs can there be used? Or what does this effect if only one LiDAR is used? Is needed to scan harder, or fly longer to obtain a good point cloud? With the three different environments simulated under nine configurations, it is possible to understand these trade-off factors.

Scanning harder or flying longer?

Based on the evaluation metric and visualization analysis, a trade-off between *scanning harder* or *flying longer* has to be chosen. There is a definite scope of adding additional LiDARs. And if addition of LiDARs is not feasible, the orientation of LiDAR and the number of laser beams used, does play a significant role. Addition of LiDARs, does come at an additional cost of power consumption, design restrictions, and user requirements. With advancement in technology, these problems can be reduced, but should be prioritized according to the user requirement and environment complexity. Flight time, and payload becomes an essential evaluation when considering the power consumption. A trade-off is established then between flying longer, as in a complex trajectory resulting in more flight time, or scanning harder, by increasing the lasers or LiDARs. By scanning harder thereby increasing the visibility and point cloud quality from the LiDAR(s), it will allow for the platform to follow a simpler trajectory, with a shorter flight path for mapping the environment. On the other hand, reducing the visibility seen from the LiDARs will require for a longer, complex trajectory. A complex trajectory requires ease in maneuverability. And a simpler trajectory requires analysis of occluded regions.

The performance of the point cloud quality varies across different environments depending on the configuration and complexity of the environment. The presented evaluation metric does not fully reflect all the quality of a point cloud. Other factors such as computational complexity, geometric quality of reconstruction, level of detailing with different lighting, trajectory trials, are equally important in evaluating the performance for indoor mapping. But the presented evaluation metric can be used as a guideline for initial testing. It has shown to provide optimistic results across a different spectrum of environments with various configurations.

6.2 Complexity and Limitations

The complexity of the algorithm is limited to identifying the nearest neighbours. Assuming a linear search, the computational complexity is $f(n)$, and additional cost of $f(1)$ is added for the calculation of threshold. This increases the load on the system. Also with the calculation of Euclidean distance between the two point clouds, it becomes vulnerable to distorted point clouds which are translated or scaled.

A limitation of the evaluation is also the manually constructed point clouds, using the collision of the models present in the environment. It is used as an indirect indicator for the evaluation of performance of coverage. It demands that the reference point cloud contain more points than the simulated point cloud. The environments considered are static. And the mobile platform is restricted to 2DoF. Additional degree of freedom will directly effect the point cloud quality obtained. The simulation are treated noise free, but in reality sensors are not noiseless. Noisy point cloud will require pre-processing directly effecting the quality of the point cloud obtained. The subsection of roof, not considered for analysis, (but simulated during data capturing) can be analysed individually, if the application demands for clear visual from top of the mobile platform. An essential limitation understood during the analysis was integration of the visual analysis of the point cloud in the evaluation metric.

6.3 Future work

Future works can consider exploring the limitations listed previously. A dynamic environment, such as a disaster site can be explored. The point cloud can evaluate the integrity of the foundation of the buildings. The coverage algorithm will need to include dynamic detection and distinguish external and internal similarities of object. Another goal to pursue worth while would be detecting the regions of trajectory that record the lowest local point density. This can help improve in trajectory planning. Inclusion of SLAM, and feature detection for different configurations is another potential direction. If SLAM algorithm are used in conjunction with the system, it could be useful to compare the trajectory error with the different configurations. This would not be a possibility in real world, and will have to integrate the simulator. A limitation to overcome to make the evaluation metric more ro-

bust, would be to include visual analysis as a qualitative score in the evaluation. This can be termed as the visibility of the point cloud, and can be according to the subsections of the environments or a few chosen features in the environment.

Chapter 7

Conclusion

The insights about the viability of incorporating several LiDAR designs on a mobile platform for mapping indoor environments are presented and discussed. The state-of-the-art compact mobile platform during study revealed a pattern of only using one "fan-styled" LiDAR. The backpack systems employing multi-LiDAR systems, showed positive results for the inclusion. Inspiration was drawn from the different available mobile mapping platforms, to design *nine* different configurations. These configurations varied in terms on number and type of LiDARs used along with their orientation, and scanner properties. A simulation tool (ROS) was used to build the pipeline for experimental collection of point cloud data by the various configurations in various environments. The evaluation of the obtained point cloud quality was based on the curated evaluation metric. The evaluation metric measured the *nominal point density*, *homogeneity score* and *coverage* of the simulated point through comparison with a manually constructed point cloud of the collision environment. The results show that the performance of the configurations varies across different environments. Generally *Tier 3*, consisted of an optimal choice of configuration. It was observed, a high coverage, NPD and homogeneity score did not necessarily provide a good configuration, the visual analysis is an important factor that has to be taken under consideration while deciding, as well as the division of the environments into further subsections, can provide a more detailed analysis. This came across as a limitation of the metric. Other factors, such as cost, power consumption and design restrictions have to be considered as well for the user/application requirements. A high coverage does not directly translate to a high NPD or homogeneity score or vice versa. A change in one, might effect the other, but the factors have to be considered as individuals during design and selection. The findings of a quantitative evaluation have been presented along with visual examples and qualitative analysis. For identifying innovative combinations, the designed evaluation metric offers a good starting point. Additionally, a significant trade-off between flying farther and scanning more completely is understood. The design and viability of the configuration are strongly influenced by this trade-off.

7.1 Summary of Research Contribution

The motivation for this project originated with the improvement in LiDAR technology such as single photon LiDAR, can there be more number of LiDARs mounted on the platform, and what would be an optimal configuration, if there is any. This led to question an important understanding of a trade-off between scanning harder or flying longer. The research contribution aim towards building an answer to these questions. To begin the analysis, it was essential to review existing LiDAR systems, as done in section 2.3. Review of these LiDAR systems, show the common configurations used by an aerial platform is of a single LiDAR, and commonly backpacks use multiple LiDAR configurations. Section 2.2 identifies the commonly used LiDAR on an aerial platform. New designs of the LiDAR systems are proposed in section 2.4. The designs are divided into 3 *Tiers* according the number of LiDARs. These designs are evaluated against an evaluation metric proposed and developed in section 3.2. The next contribution, section 4.2, is building a tool to simulate the proposed designs/configurations, along with selection of the environments. Each environment is explored, with the new proposed designs, and point clouds obtained are compared to one other. Warehouse is a small environment, the point cloud obtained do not provide sufficient aspects for analysis, as discussed in section 5.1.3. The medical camp is a bigger organized environment. and provides a better insight in the differences between the configurations, discussed in section 5.2.3. An interesting path to explore was the dependency of the range and orientation of the LiDAR of the quality of the point cloud, this is explored in section 5.2.4. Generally, a mid-range sensor with an inclined orientation provides a better point cloud quality. The forest environment, is a very different exploration. It is an unorganized indoor environment, which can be compared to a tunnel or cave, spaces which are cramped, and require the platform at a lower height level. This environment, provided interesting analysis on the configurations, as seen in section 5.3.3. The designs which were good for the previous environments, performed poorly in this one. An overall, comparative analysis is discussed under section 6.1, with a critical view on the initial question.

References

- [1] Martin Velas et al.
“Indoor and Outdoor Backpack Mapping with Calibrated Pair of Velodyne LiDARs”.
In: *Sensors* 19.18 (Sept. 2019), p. 3944. DOI: 10.3390/s19183944.
URL: <https://doi.org/10.3390/s19183944>.
- [2] Thinal Raj et al. “A Survey on LiDAR Scanning Mechanisms”.
In: *Electronics* 9.5 (Apr. 2020), p. 741. DOI: 10.3390/electronics9050741.
URL: <https://doi.org/10.3390/electronics9050741>.
- [3] Tao Yang et al. *3D ToF LiDAR in Mobile Robotics: A Review*. 2022.
DOI: 10.48550/ARXIV.2202.11025. URL: <https://arxiv.org/abs/2202.11025>.
- [4] S. Karam, V. Lehtola, and G. Vosselman.
“STRATEGIES TO INTEGRATE IMU AND LIDAR SLAM FOR INDOOR MAPPING”.
In: *ISPRS Annals of the Photogrammetry, Remote Sensing and Spatial Information Sciences* V-1-2020 (Aug. 2020), pp. 223–230.
DOI: 10.5194/isprs-annals-v-1-2020-223-2020.
URL: <https://doi.org/10.5194/isprs-annals-v-1-2020-223-2020>.
- [5] Vectornav. *GEOREFERENCING LIDAR DATA*.
URL: <https://www.vectornav.com/applications/lidar-mapping>.
- [6] H. Andrew Lassiter et al. “Scan Pattern Characterization of Velodyne VLP-16 Lidar Sensor for UAS Laser Scanning”. In: *Sensors* 20.24 (Dec. 2020), p. 7351.
DOI: 10.3390/s20247351. URL: <https://doi.org/10.3390/s20247351>.
- [7] Kouros Khoshelham et al. “Results of the ISPRS benchmark on indoor modelling”.
In: *ISPRS Open Journal of Photogrammetry and Remote Sensing* 2 (Dec. 2021),
p. 100008. DOI: 10.1016/j.ophoto.2021.100008.
URL: <https://doi.org/10.1016/j.ophoto.2021.100008>.
- [8] Ville Lehtola et al. “Comparison of the Selected State-Of-The-Art 3D Indoor Scanning and Point Cloud Generation Methods”. In: *Remote Sensing* 9.8 (Aug. 2017), p. 796.
DOI: 10.3390/rs9080796. URL: <https://doi.org/10.3390/rs9080796>.

-
- [9] Dong Tian et al. “Geometric distortion metrics for point cloud compression”. In: *2017 IEEE International Conference on Image Processing (ICIP)*. IEEE. 2017, pp. 3460–3464.
- [10] Evangelos Alexiou and Touradj Ebrahimi. “Point Cloud Quality Assessment Metric Based on Angular Similarity”. In: *2018 IEEE International Conference on Multimedia and Expo (ICME)*. 2018, pp. 1–6. DOI: 10.1109/ICME.2018.8486512.
- [11] Hyun-Jae Yoo et al. “Simulation based comparative analysis for the design of laser terrestrial mobile mapping systems”. In: *Bulletin of Geodetic Sciences* 15.5 (2009).
- [12] Conor Cahalane et al. “Optimising Mobile Mapping System Laser Scanner Orientation”. In: *ISPRS International Journal of Geo-Information* 4.1 (Feb. 2015), pp. 302–319. DOI: 10.3390/ijgi4010302. URL: <https://doi.org/10.3390/ijgi4010302>.
- [13] Minkyung Chung et al. “Development of LiDAR simulator for backpack-mounted mobile indoor mapping system”. In: *Journal of the Korean Society of Surveying, Geodesy, Photogrammetry and Cartography* 35.2 (2017), pp. 91–102.
- [14] Antero Kukko et al. “Graph SLAM correction for single scanner MLS forest data under boreal forest canopy”. In: *Isprs Journal of Photogrammetry and Remote Sensing* 132 (2017), pp. 199–209.
- [15] Dataspeed Inc. *Velodyne_simulator*. URL: http://wiki.ros.org/velodyne_simulator.
- [16] Samer Karam et al. “Design, Calibration, and Evaluation of a Backpack Indoor Mobile Mapping System”. In: *Remote. Sens.* 11 (2019), p. 905.